Relevance of the Electronegativity of Boron in η^5-Coordinating Ligands: Regioselective Monoalkylation and Monoarylation in Cobaltabisdicarbollide $[3,3'\text{-}Co(1,2\text{-}C_2B_9H_{11})_2]^-$ Clusters

Isabel Rojo,[a] Francesc Teixidor,*[a] Clara Viñas,[a] Raikko Kivekäs,[b] and Reijo Sillanpää[c]

Abstract: Regioselective monoalkylation and monoarylation in cobaltabisdicarbollide clusters has been achieved starting from $Cs[8\text{-}I\text{-}3,3'\text{-}Co(1,2\text{-}C_2B_9H_{10})(1',2'\text{-}C_2B_9H_{11})]$ by cross-coupling reactions between a B–I fragment and an appropriate Grignard reagent in the presence of a Pd catalyst and CuI. A considerable number of monoalkylated and monoarylated derivatives have been synthesized, which allowed study of the influence of boron in metallocene-type ligands and the effect of alkyl and aryl substituents on boron in boron anionic clusters. Experimental data from UV/Vis spectroscopy, $E_{1/2}$ measurements, and X-ray diffraction analysis, and supported by EHMO and ab initio analyses, indicate that the participation of metal d orbitals in the HOMO is less than that in typical metallocene complexes. This can be explained in terms of the lower electronegativity of boron compared to carbon. Related to this is the –I character of alkyl groups when bonded to boron in boron anionic clusters, contrary to the common belief that alkyl groups are generally electron-releasing moieties.

Keywords: cobalt · B–C coupling · charge transfer · cross-coupling · isolobal relationship

Introduction

The cyclopentadienyl ligand, $[C_5H_5]^-$, produces "half-sandwich" and "sandwich" compounds, metallocenes that occur widely in contemporary organometallic chemistry. It is usually assumed that for generic metallocenes the six lowest orbitals are based mainly on the contributions of the $[C_5H_5]^-$ orbitals and that the next five MOs have little or no bonding character.[1] This orbital diagram can be modulated on going to substituted $[C_5H_5]^-$ derivatives. In this sense, the pentamethylcyclopentadienyl, $[C_5Me_5]^-$ or Cp*, is one of the best known, allowing the isolation of Cp* complexes for which $[C_5H_5]^-$ analogues are unknown or are kinetically unstable.[2] The methyl groups on Cp* are electron-releasing, and this results in more electron density at the metal than in the analogous $[C_5H_5]^-$ complexes. Accordingly, electrochemical measurements indicate that Cp* complexes are more easily oxidized than the $[C_5H_5]^-$ analogues by approximately 0.5 V.[1] Other examples of $[C_5H_5]^-$ derivatives include C_5Me_4H,[3] C_5H_4Me,[4] and the important class of indenyl complexes.[5] More profound changes are obtained by replacing a carbon by nitrogen, as in the structurally analogous pyrrolyl anion $[NC_4H_4]^-$.[6] Similarly to $[C_5H_5]^-$, more stable ligand molecular orbitals are generated, due to the higher electronegativity of nitrogen.[7, 8] In this case, the nonbonding character of the metal d orbitals should be even more enhanced than that in $[C_5H_5]^-$ metallocenes. The question that arises is whether this situation can be reversed. We hypothesized that the incorporation of the less electronegative boron in the ring should produce a different situation.

Recently, alkyl substitution on boron in boron clusters has become a subject of renewed interest. Alkylations with different degrees of alkyl incorporation have been performed on $[B_{12}H_{12}]^{2-}$,[9] $[CB_{11}H_{11}]^-$,[10] $p\text{-}C_2B_{10}H_{12}$,[11] $m\text{-}C_2B_{10}H_{12}$,[12]

[a] Dr. F. Teixidor, I. Rojo,[+] Dr. C. Viñas
Institut de Ciència de Materials de Barcelona (C.S.I.C.)
Campus de la U.A.B., 08193 Bellaterra (Spain)
Fax: +34 (9)-3-5805729
E-mail: teixidor@icmab.es

[b] R. Kivekäs
Department of Chemistry, P.O. Box 55
University of Helsinki
00014 Helsinki (Finland)

[c] R. Sillanpää
Department of Chemistry, University of Jyväskylä
40351 Jyväskylä (Finland)

[+] I. Rojo
Isabel Rojo is enrolled in the Ph.D. program of the UAB.

Supporting information for this article is available on the WWW under http://www.chemeurj.org or from the author: ^1H and $^{13}C\{^1H\}$ NMR spectra for compounds $[\mathbf{2}]^- - [\mathbf{9}]^-$.

 DOI: 10.1002/chem.200304970

and *o*-$C_2B_{10}H_{12}$.[13] Except in the case of *o*-carborane, alkylation procedures have been directed towards permethylation by using strong methylating agents such as MeI/$AlCl_3$[12] or CF_3SO_3Me.[11, 14] In the case of *o*-carborane, selective alkylations/arylations at positions 9, 12 or 3 have been successfully achieved from the corresponding iodo derivatives.[15] However, the derivative chemistry of the most extensively studied of the anionic borate clusters, the cobaltabisdicarbollide [3,3′-Co(1,2-$C_2B_9H_{11}$)$_2$]$^-$ ([**1**]$^-$), remains very much unexplored.[16] The fundamental reason for this is the synthetic strategy leading to these derivatives. Two basic substitutions may occur on [**1**]$^-$, on either carbon or boron. With few exceptions,[17] substitutions on carbon have been achieved at a very early stage on the starting *o*-carborane,[18] and therefore [**1**]$^-$ has not been used as starting material. Substitution on boron has been achieved under Friedel–Crafts conditions[19] or with strong alkylating agents.[20] Consequently, regioselective substitutions have not been possible, and specific derivatives could only be obtained after careful separations of complex mixtures. Very recently, the facile, high-yielding preparation of the zwitterionic 8-dioxanate derivative [8-$C_4H_8O_2$-3,3′-Co(1,2-$C_2B_9H_{10}$)(1′,2′-$C_2B_9H_{11}$)][21] has facilitated the preparation of many derivatives of [**1**]$^-$ by nucleophilic ring opening.[22] An alternative starting material is [8-OH-3,3′-Co(1,2-$C_2B_9H_{10}$)(1′,2′-$C_2B_9H_{11}$)]$^-$.[23] Besides these remarkable compounds, there are the readily available halogeno derivatives of [**1**]$^-$.[24] In this regard, regiospecific syntheses of 8-I and 8,8′-I_2[25] have been described, but no 8-alkyl/aryl derivatives have been reported. As mentioned by Bregadze in 1992,[26] halogeno derivatives appear to be inert towards substitution reactions, although Hawthorne and co-workers have recently shown that starting from [3,3′-Co(8,9,12-I_3-1,2-$C_2B_9H_8$)$_2$]$^-$ it is possible to achieve the hexasubstitution of [**1**]$^-$.[27] This opened up the possibility of achieving monosubstitution from [8-I-3,3′-Co(1,2-$C_2B_9H_{10}$)(1′,2′-$C_2B_9H_{11}$)]$^-$ ([**2**]$^-$). Figure 1 shows the numbering of the vertices for compound [**2**]$^-$.

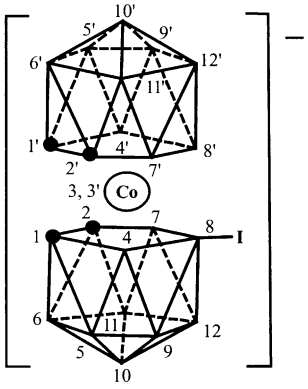

Figure 1. Numbering of the vertices for [8-I-3,3′-Co(1,2-$C_2B_9H_{10}$)(1′,2′-$C_2B_9H_{11}$)]$^-$ ([**2**]$^-$).

In this report, we describe how the latter compound, [**2**]$^-$, can be a suitable starting material for regiospecifically obtaining alkyl and aryl derivatives of [**1**]$^-$ and, with the compounds in hand, how we were able to study the effect of alkyl or aryl substitution on their electronic properties.

Results

Modified synthesis of Cs[8-I-3,3′-Co(1,2-$C_2B_9H_{10}$)(1′,2′-$C_2B_9H_{11}$)] (Cs[2]): Matel and co-workers[25] reported a method whereby [**1**]$^-$ could be quantitatively converted into the corresponding B8-monoiodinated compound ([**2**]$^-$). However, during our investigation we found that on applying the same procedure a mixture of the starting compound [**1**]$^-$ and the desired product [**2**]$^-$ was obtained. Therefore, we have slightly modified the reported procedure so as to obtain [**2**]$^-$ as a pure compound (see Experimental Section). Under our new reaction conditions, we were able to increase the yield from 84% in the reported reaction to 95%, and our work-up procedure is shorter.

Palladium-catalyzed B–C cross-coupling reactions on Cs[8-I-3,3′-Co(1,2-$C_2B_9H_{10}$)(1′,2′-$C_2B_9H_{11}$)] with Grignard reagents: We were interested in checking whether the cross-coupling methodology that can be successfully used at the antipodal, B9, and/or B12 *o*-carborane positions[15a,b] of 9,12-I_2-1,2-$C_2B_{10}H_{10}$ and 12-I-1,2-$C_2B_{10}H_{11}$, at the B3 vertex of 3-I-1,2-$C_2B_{10}H_{11}$, and at B8, B9, and B12[27] of the [3,3′-Co(8,9,12-I_3-$C_2B_9H_8$)$_2$]$^-$ could also be applied at the single B8 vertex of [8-I-3,3′-Co(1,2-$C_2B_9H_{10}$)(1′,2′-$C_2B_9H_{11}$)]$^-$. Successful B–C coupling reaction was achieved by using Cs[8-I-3,3′-Co(1,2-$C_2B_9H_{10}$)(1′,2′-$C_2B_9H_{11}$)] (Cs[**2**]) as the starting compound. The B–I unit was transformed into a B–R vertex by using a Grignard reagent in the presence of a palladium catalyst and copper(I) iodide as a cocatalyst.[15a] In a typical experiment, the Cs[**2**] salt was dissolved in THF and treated with the Grignard reagent at low temperatures (Scheme 1). A range of temperatures between −84 and 0 °C was typically investigated. A

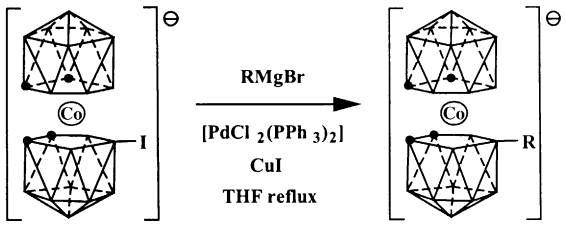

R = I ([**2**]$^-$)
R = Methyl ([**3**]$^-$)
R = Ethyl ([**4**]$^-$)
R = Phenyl ([**5**]$^-$)
R = Biphenyl ([**6**]$^-$)
R = Anthracenyl ([**7**]$^-$)
R = 4-Butylphenyl ([**8**]$^-$)
R = 2-Phenylethyl ([**9**]$^-$)

Scheme 1.

brown precipitate formed; the mixture was then allowed to warm to room temperature, whereupon the palladium catalyst and CuI were added in a single portion. A period of reflux, ranging from a few minutes to several hours, followed by work-up, yielded the desired compounds. The reaction provided good to very good yields of all the compounds (between 76 and 95%). The reaction seems to be quite general, once the optimal conditions in terms of temperature

and reaction time have been found. The versatility of the reaction has been explored by producing B8–alkyl (methyl [**3**]$^-$, ethyl [**4**]$^-$), B8–aryl (phenyl [**5**]$^-$, biphenyl [**6**]$^-$, anthracenyl [**7**]$^-$), combined aryl/alkyl (4-butylphenyl ([**8**]$^-$)), and combined alkyl/aryl (2-phenylethyl ([**9**]$^-$)) derivatives. Thus, it can be considered a general reaction for the regioselective generation of 8-alkyl or 8-aryl derivatives of compound [**1**]$^-$.

The Pd-catalyzed coupling of [**2**]$^-$ with Grignard reagents described here is proposed to follow the mechanistic pathway previously proposed for the similar Pd-catalyzed coupling of Grignard reagents with *B*-iodocarborane derivatives.[15a, 28] In these earlier reports, it was said that diminished yields are observed in reactions in which the intermediate in the catalytic cycle is capable of β-hydrogen elimination. If this were the case, low coupling yields would have been expected with ethylmagnesium bromide, but the corresponding product was obtained in reasonably good yield (80%). However, β-hydrogen elimination may account for the unsuccessful preparations of [8-CH_2=$CHCH_2$-3,3′-Co(1,2-$C_2B_9H_{10}$)-(1′,2′-$C_2B_9H_{11}$)]$^-$, [8-Cl$(CH_2)_3$-3,3′-Co(1,2-$C_2B_9H_{10}$)(1′,2′-$C_2B_9H_{11}$)]$^-$, [8-CH_2=$CH(CH_2)_3$-3,3′-Co(1,2-$C_2B_9H_{10}$)(1′,2′-$C_2B_9H_{11}$)]$^-$, and [8-Me$(CH_2)_9$-3,3′-Co(1,2-$C_2B_9H_{10}$)(1′,2′-$C_2B_9H_{11}$)]$^-$. Attempts to synthesize these compounds were made by reacting the cesium salt of [**2**]$^-$ with allylmagnesium bromide or with the corresponding Grignard reagents of 1-chloro-3-iodopropane, 5-bromopentene, and 1-bromodecane, respectively. The nature of [**3**]$^-$–[**9**]$^-$ has been corroborated by elemental analysis, MS, IR, and ^{1}H, ^{1}H{^{11}B}, ^{13}C{^{1}H}, ^{11}B, and ^{11}B{^{1}H} NMR spectroscopies, and where appropriate, for [*n*Bu_4N][**3**], [Me_4N][**8**], and [Me_4N][**9**], by X-ray crystal structure determination.

NMR spectral considerations

Qualitative description of the ^{11}B NMR spectra: The sensitivity of the electron distribution in carboranes to the presence of substituents has long been apparent.[29] For icosahedral carborane derivatives of 1-R-1,2-*closo*-$C_2B_{10}H_{11}$, ^{11}B NMR studies have shown that the chemical shifts of the cage boron atoms vary with the substituent R,[30] particularly that at the boron atom opposite to the point of attachment of the substituent, the "antipodal atom".[30b, 31] In this work, we report compounds with a substituent on the B8 atom of cobaltabisdicarbollide and the influence of this substituent on the ^{11}B chemical shift.

The ^{11}B{^{1}H} NMR data of [**1**]$^-$, [**2**]$^-$, and all of the monosubstituted compounds prepared in this work are shown in Table 1. The spectra can be interpreted considering the ^{11}B{^{1}H} NMR spectra of [**1**]$^-$ and [**2**]$^-$, the latter also being derived from [**1**]$^-$. The ^{11}B{^{1}H} NMR spectrum of [**1**]$^-$ displays five resonances in the range $\delta = +6.5$ to $\delta = -22.7$ with a 2:2:8:4:2 pattern, in agreement with an averaged C_{2v} symmetry. The ^{11}B NMR chemical shifts of compound [**1**]$^-$ were assigned with the aid of a 2D ^{11}B{^{1}H}-^{11}B{^{1}H} COSY experiment and correspond to B(8,8′), B(10,10′), B(4,4′,7,7′,9,9′,12,12′), B(5,5′,11,11′), and B(6,6′) from low to high field.[32] Incorporation of one iodine atom at position B8 lowers the symmetry to C_s, maintaining only one symmetry plane and rendering the two dicarbollide moieties non-equivalent. Therefore, the ^{11}B{^{1}H} NMR spectrum of [**2**]$^-$ displays ten resonances in the range $\delta = +6.5$ to $\delta = -23.1$, with a 1:1:1:2:*5*:2:2:2:1:1 pattern. The resonance in italics integrating as five corresponds to the B–I signal, which overlaps with four B–H signals.

Substitution of iodine by alkyl and aryl groups maintains the same C_s symmetry and therefore the observed pattern is almost the same. In Table 1, the B–C resonance is shown in italics. The rather complex ^{11}B{^{1}H} spectra of [3,3′-Co(1,2-$C_2B_9H_{11})_2$]$^-$ derivatives with a B8–C bond consist of one set of signals for each carborane ligand moiety, one perturbed by B–C substitution and the second almost unchanged compared to that of parent unsubstituted anion [**1**]$^-$. Only when no peak coincidence overlap was found could the positions be assigned

Table 1. ^{11}B{^{1}H} NMR spectra [ppm] of B8-monosubstituted derivatives of [3,3′-Co(1,2-$C_2B_9H_{11})_2$]$^-$. Within each column, the number of boron atoms shown in the first entry (the parent compound) is preserved. An asterisk (*) is used to denote where one of the two boron atoms should be accounted for in the following column. Figures in italics relate to the resonances due to B–R (R ≠ H). The numbers in parentheses denote coupling constants ^1J(B,H) in Hertz.

Compound	δ^{11}B Integration											
[**1**]	**6.5** 2		**1.4** 2		**–6.0** 8		**–17.2** 4		**–22.7** 2			
[**2**]$^-$	**6.5** 1	**3.5** 1	**1.3** 1	**–1.7** 2*	***–4.8*** *5*	**–5.4** 2	**–16.0** 2	**–17.5** 2	**–20.9** 1	**–23.1** 1		
	(138)	(154)	(157)	(151)	(135)	(140)	(145)	(147)	(186)	(188)		
[**3**]$^-$	***16.6*** *1*	**7.6** 1	**0.6** 2		**–3.5** 2	**–4.7** 4	**–6.2** 2	**–17.3** 2	**–17.8** 2	**–22.3** 1	**–25.3** 1	
		(142)	(140)		(138)	(120)	(138)	(144)	(148)	(172)	(169)	
[**4**]$^-$	***19.0*** *1*	**7.8** 1	**1.2** 2		**–4.7** 6		**–5.7** 2	**–16.7** 4		**–21.6**	**–24.4** 1	
		(140)	(137)		(107)		(118)	(149)		(183)	(178)	
[**5**]$^-$	***13.3*** *1*	**5.7** 1	**2.5** 2		**–2.8** 2	**–4.6** 4	**–6.1** 2	**–16.6** 2	**–17.9** 2	**–21.2** 1	**–22.3** 1	
		(134)	(127)		(168)	(148)	(141)	(138)	(135)	(121)	(130)	
[**6**]$^-$	***13.3*** *1*	**6.2** 1	**2.6** 2		**–2.7** 2	**–4.3** 4	**–5.9** 2	**–16.5** 2	**–17.7** 2	**–21.1** 1	**–22.2** 1	
		(155)	(132)		(147)	(143)	(149)	(92)	(136)	(104)	(156)	
[**7**]$^-$	***11.3*** *1*	**5.3** 1	**2.2** 1	**1.4** 1	**–2.8** 2	**–4.7** 4	**–6.2** 2	**–16.9** 4		**–20.8** 2		
		(138)	(103)	(118)	(184)	(143)	(140)	(151)		(158)		
[**8**]$^-$	***11.8*** *1*	**3.7** 1	**1.1** 1	**0.7** 1	**–4.2** 2	**–6.2** 4	**–7.7** 2	**–18.3** 2	**–19.5** 2	**–22.5** 1	**–23.9** 1	
		(137)	(136)	(136)	(154)	(146)	(145)	(139)	(141)	(145)	(122)	
[**9**]$^-$	***16.3*** *1*	**6.5** 1	**2.5** 2		**–6.0** 6		**–7.1** 2	**–18.3** 4		**–23.4** 1	**–25.8** 1	
		(137)	(136)		(146)		(145)	(139)		(145)	(122)	

on the basis of cross-peaks in the $^{11}B\{^1H\}$-$^{11}B\{^1H\}$ COSY experiments. The resonance at $\delta = +16.6$ is not split into a doublet in the ^{11}B NMR spectrum of compound $[\mathbf{3}]^-$, indicating that this resonance corresponds to the B–Me vertex (Figure 2). Once the B8 resonance was known, the two-dimensional $^{11}B\{^1H\}$-$^{11}B\{^1H\}$ COSY NMR spectrum proved helpful for the assignment of the remaining peaks.[33]

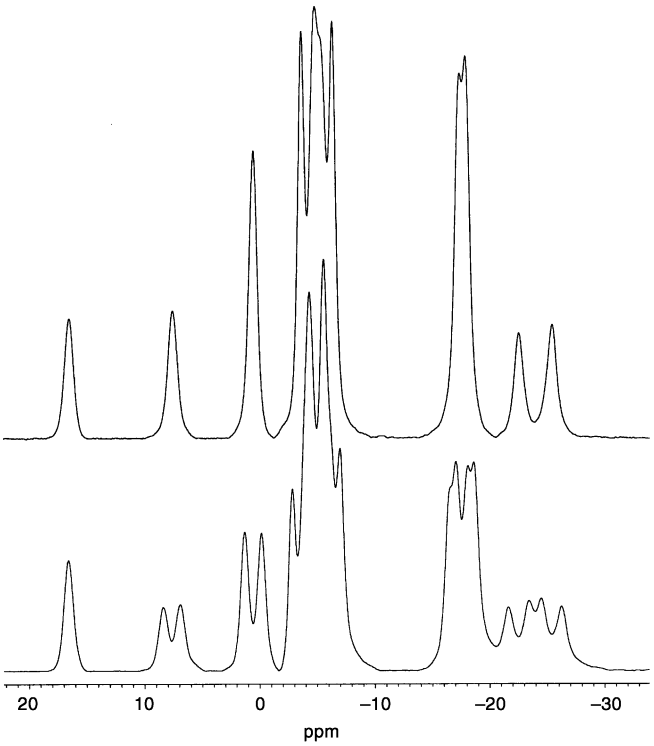

Figure 2. $^{11}B\{^1H\}$ and ^{11}B NMR spectra of $[n\mathrm{Bu_4N}][8\text{-Me-}3,3'\text{-Co}(1,2\text{-}C_2B_9H_{10})(1',2'\text{-}C_2B_9H_{11})]$.

Figure 3 shows the $^{11}B\{^1H\}$ NMR and $^{11}B\{^1H\}$-$^{11}B\{^1H\}$ COSY NMR spectra of compound $[\mathbf{3}]^-$, with the assignments deduced from the off-diagonal resonances. A stick representation of the chemical shifts and relative intensities in the $^{11}B\{^1H\}$ NMR spectra of compounds $[\mathbf{1}]^-$ and $[\mathbf{3}]^-$ is shown in Figure 4. Compared with compound $[\mathbf{1}]^-$, compound $[\mathbf{3}]^-$ shows a 10 ppm deshielding at B8, the vertex bonded to the methyl group, and a 2.5 ppm deshielding at the B4 and B7 positions, these being adjacent to B8. There is also a shielding effect of 2.6 ppm at B6, which is the antipodal vertex to B(8). Table 2 shows the boron NMR data for compounds $[\mathbf{1}]^-$ and $[\mathbf{3}]^-$.

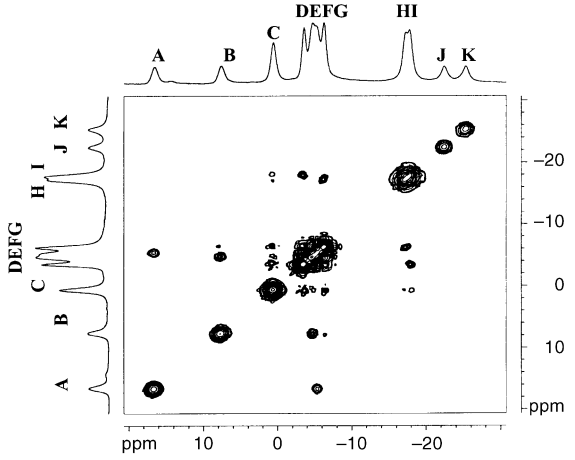

Figure 3. The $^{11}B\{^1H\}$-$^{11}B\{^1H\}$ 2D COSY NMR spectrum of $[n\mathrm{Bu_4N}][8\text{-Me-}3,3'\text{-Co}(1,2\text{-}C_2B_9H_{10})(1',2'\text{-}C_2B_9H_{11})]$. The resonance marked **A** corresponds to B8, **B** to B8′, **C** to B(10,10′), **D** to B(4,7), **E** to B(4′,7′), **F** to B(8,12), **G** to B(9′,12′), **H** to B(5′,11′), **I** to B(5,11), and **J** and **K** to B6 and B6′.

Table 2. $^{11}B\{^1H\}$ NMR chemical shifts [ppm] for compounds $Cs[3,3'\text{-}Co(1,2\text{-}C_2B_9H_{11})_2]$ and $[n\mathrm{Bu_4N}][8\text{-Me-}3,3'\text{-Co}(1,2\text{-}C_2B_9H_{10})(1',2'\text{-}C_2B_9H_{11})]$. $\Delta\delta$ are the differences between the chemical shift of $[n\mathrm{Bu_4N}][8\text{-Me-}3,3'\text{-Co}(1,2\text{-}C_2B_9H_{10})(1',2'\text{-}C_2B_9H_{11})]$ and that of the same vertex in $Cs[3,3'\text{-Co}(1,2\text{-}C_2B_9H_{11})_2]$.

Boron atom	$[\mathbf{1}]^-$	$[\mathbf{3}]^-$	$\Delta\delta$
B8	6.5	16.6	$16.6-(6.5)=+\mathbf{10.1}$
B8′	6.5	7.6	$7.6-(6.5)=+1.1$
B10,B10′	1.4	0.6	$0.6-(1.4)=-0.8$
B4,B7	−6.0	−3.5	$-3.5-(-6.0)=+\mathbf{2.5}$
B4′,B7′	−6.0	−4.7	$-4.7-(-6.0)=+1.3$
B9,B12	−6.0	−4.7	$-4.7-(-6.0)=+1.3$
B9′,B12′	−6.0	−6.2	$-6.2-(-6.0)=-0.2$
B5′,B11′	−17.2	−17.3	$-17.3-(-17.2)=-0.1$
B5,B11	−17.2	−17.8	$-17.8-(-17.2)=-0.6$
B6′	−22.7	−22.4	$-22.4-(-22.7)=+0.3$
B6	−22.7	−25.3	$-25.3-(-22.7)=-\mathbf{2.4}$

Qualitative description of ^1H and $^{13}C\{^1H\}$ NMR spectra: In agreement with the symmetry, the ^1H and $^{13}C\{^1H\}$ NMR spectra exhibit two slightly different C–H carborane signals ($C_{cluster}$–H) due to the substituted and the unsubstituted cage for $[\mathbf{2}]^- - [\mathbf{9}]^-$ (Table 3), and one C–H carborane signal for $[\mathbf{1}]^-$. They also display resonances attributable to the R groups at the expected positions.

Table 3. Chemical shift values [ppm] of the hydrogen and carbon cluster atoms in the ^1H and $^{13}C\{^1H\}$ NMR spectra of B(8)-monosubstituted derivatives of $[3,3'\text{-Co}(1,2\text{-}C_2B_9H_{11})_2]^-$.

Compound	δ $^{13}C\{^1H\}$ NMR	δ ^1H NMR
$[\mathbf{1}]^-$	51.03	3.94 (brs, 4H)
$[\mathbf{2}]^-$	59.34	4.54 (brs, 2H)
	49.16	4.29 (brs, 2H)
$[\mathbf{3}]^-$	51.03	4.08 (brs, 2H)
	49.87	3.87 (brs, 2H)
$[\mathbf{4}]^-$	50.55	4.10 (brs, 2H)
	49.25	3.88 (brs, 2H)
$[\mathbf{5}]^-$	54.03	4.58 (brs, 2H)
	49.76	3.76 (brs, 2H)
$[\mathbf{6}]^-$	53.75	4.60 (brs, 2H)
	49.76	3.87 (brs, 2H)
$[\mathbf{7}]^-$	53.07	4.52 (brs, 2H)
	47.82	3.08 (brs, 2H)
$[\mathbf{8}]^-$	54.40	4.60 (brs, 2H)
	49.78	3.73 (brs, 2H)
$[\mathbf{9}]^-$	50.42	4.12 (brs, 2H)
	49.14	3.92 (brs, 2H)

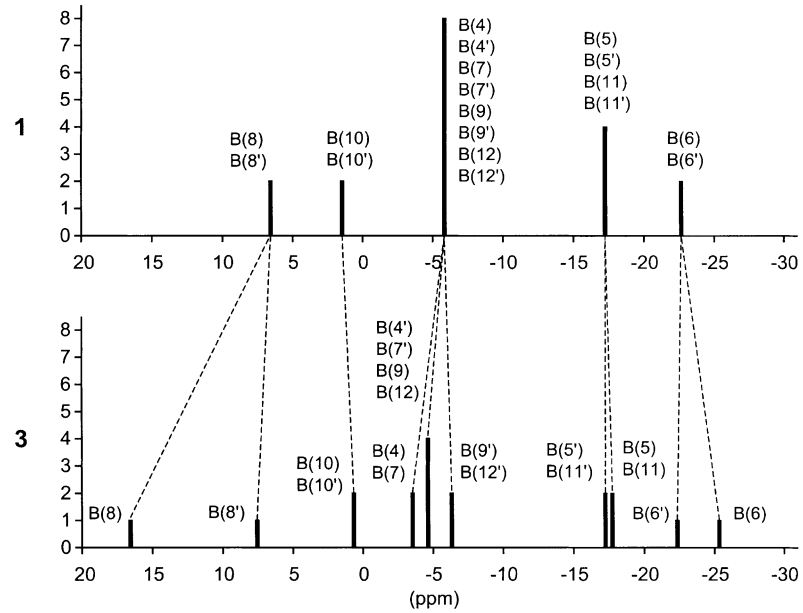

Figure 4. Stick representation of the chemical shifts and relative intensities in the $^{11}B\{^1H\}$ NMR spectra of compounds $[\mathbf{1}]^-$ and $[\mathbf{3}]^-$. Lines join equivalent positions in the two compounds.

Molecular and crystal structures of $[\mathbf{3}]^-$, $[\mathbf{8}]^-$, and $[\mathbf{9}]^-$: Suitable single crystals of $[\mathbf{3}]^-$ were obtained by slow evaporation of the solvents from a solution in $CHCl_3$/hexane. In the case of $[\mathbf{8}]^-$, crystals were obtained by slow concentration of a solution in CH_2Cl_2/acetone, while $[\mathbf{9}]^-$ was similarly crystallized from a mixture of CH_2Cl_2/EtOH/acetone.

The structures of $[\mathbf{3}]^-$, $[\mathbf{8}]^-$, and $[\mathbf{9}]^-$ are presented in Figures 5–7, respectively. Crystallographic data for $[n\mathrm{Bu_4N}][\mathbf{3}]$, $[\mathrm{Me_4N}][\mathbf{8}]$, and $[\mathrm{Me_4N}][\mathbf{9}]$ are given in Table 4,

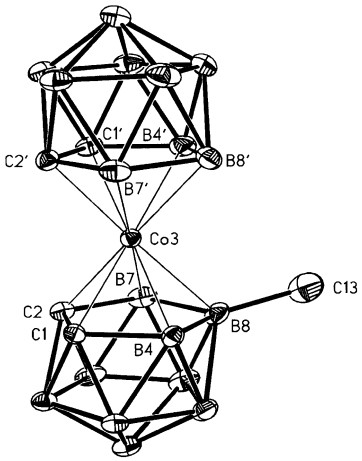

Figure 5. Drawing of $[\mathbf{3}]^-$ with 30% thermal displacement ellipsoids.

and selected bond lengths and angles are listed in Tables 5–7, respectively. Crystallographic analyses confirmed the expected B(8)-substituted cobaltabisdicarbollide structures for each compound. In each compound, the B10-Co3-B10′ jack-knife angle (see Figure 1) is close to 180° [174.98(7)–178.86(5)°] and the Co3–B8 distance is slightly longer than the Co3–C_c distances (C_c is the cluster carbon atom).

In each compound, the two five-membered coordinating sites are in a staggered conformation. The rotamers of $[\mathbf{3}]^-$ and $[\mathbf{9}]^-$ (defined by two cobaltabisdicarbollide moieties) are similar, but that of $[\mathbf{8}]^-$ is different. In $[\mathbf{3}]^-$ and $[\mathbf{9}]^-$, C2′ is oriented between C1 and C2 and thus the cluster carbon atoms of the non-substituted dicarbollide cage are oriented away from the B8 atom bearing the substituent, while in $[\mathbf{8}]^-$ B8 is oriented between C1′ and C2′. The former conformation has been observed in most cases,[22e, 34] while the latter conformation has been found in complex $[\mathbf{5}]^-$, which also bears a phenyl substituent at B8.[21] In

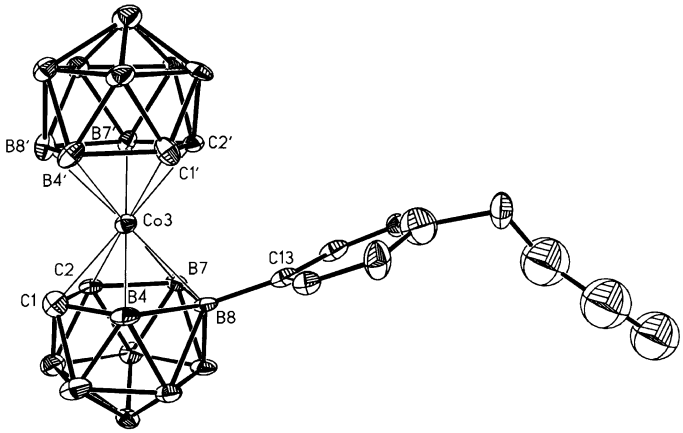

Figure 6. Drawing of $[\mathbf{8}]^-$ with 20% thermal displacement ellipsoids.

$[\mathbf{3}]^-$ and $[\mathbf{9}]^-$, the Co3-B8-C13 angles are 121.1(2) and 122.6(3)°, respectively. On the other hand, the Co3-B8-C13 angle in $[\mathbf{8}]^-$ is 114.37(13)°, which is comparable with the corresponding value of 116.9° in $[\mathbf{5}]^-$. It seems that in $[\mathbf{8}]^-$ the phenyl group at B8 is oriented towards the cobalt atom and the upper belt. Thus, the reason for the unusual rotamer may be a weak interaction between the metal atom and the phenyl group, and/or a weak interaction between the hydrogens at C1′ and C2′ and the phenyl carbon atoms.

The C1–C2 and C1′–C2′ bond lengths in $[\mathbf{3}]^-$ and $[\mathbf{9}]^-$ are similar (about 1.615 Å; see Table 5 and Table 7), but in $[\mathbf{8}]^-$ (Table 6) the corresponding distances are 1.662(3) and 1.599(3) Å, respectively. The B8–C13 distance in $[\mathbf{8}]^-$ is 1.652(3) Å, while that in $[\mathbf{5}]^-$ is 1.577(5) Å.[21] The elongated distance in the former is possibly due to the long attached alkyl group.

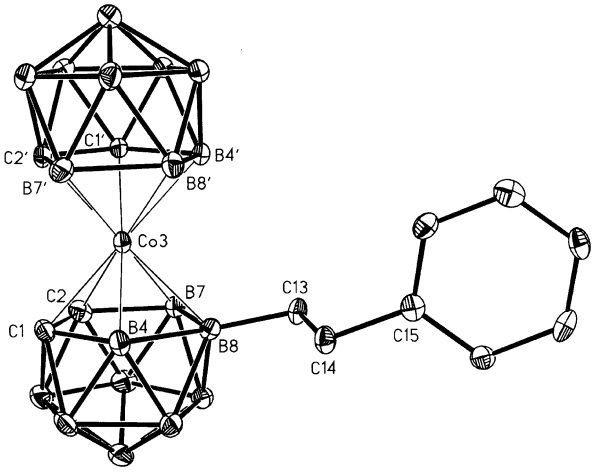

Figure 7. Drawing of $[\mathbf{9}]^-$ with 30% thermal displacement ellipsoids.

Table 4. Crystallographic data and structural refinement details for compounds $[n\mathrm{Bu_4N}][\mathbf{3}]$, $[\mathrm{Me_4N}][\mathbf{8}]$, and $[\mathrm{Me_4N}][\mathbf{9}]$.

	$[n\mathrm{Bu_4N}][\mathbf{3}]$	$[\mathrm{Me_4N}][\mathbf{8}]$	$[\mathrm{Me_4N}][\mathbf{9}]$
empirical formula	$C_{21}H_{60}B_{18}CoN$	$C_{18}H_{46}B_{18}CoN$	$C_{16}H_{42}B_{18}CoN$
formula weight	580.21	530.07	502.02
crystal system	monoclinic	monoclinic	orthorhombic
space group	$P2_1/n$ (no. 14)	Cc (no. 9)	$P2_12_12_1$ (no. 19)
a [Å]	14.7523(2)	18.6079(8)	13.8955(3)
b [Å]	10.8299(2)	17.6746(9)	13.9474(3)
c [Å]	22.2034(3)	9.9608(4)	14.4267(3)
β [°]	103.2283(7)	112.942(3)	90
V [Å^3]	3453.22(9)	3016.8(2)	2795.98(10)
Z	4	4	4
T [°C]	−100	−100	−100
λ [Å]	0.71073	0.71073	0.71073
ρ [g cm^{-3}]	1.116	1.167	1.193
μ [cm^{-1}]	5.13	5.81	6.24
goodness-of-fit	0.997	1.058	1.032
$R1$[a] $[I > 2\sigma(I)]$	0.0465	0.0778	0.0462
$wR2$[b] $[I > 2\sigma(I)]$	0.1133	0.2042	0.0876
Flack parameter x	–	0.31(7)	0.171(19)

[a] $R1 = \Sigma\,||F_o| - |F_c||/\Sigma\,|F_o|$. [b] $wR2 = \{\Sigma[w(F_o^2 - F_c^2)^2]/\Sigma[w(F_o^2)^2]\}^{1/2}$.

Table 5. Selected bond lengths [Å] and angles [°] for $[n\mathrm{Bu_4N}][\mathbf{3}]$.

Co3 – C1	2.032(2)
Co3 – C2	2.039(3)
Co3 – C1′	2.048(3)
Co3 – C2′	2.040(3)
Co3 – B8	2.144(3)
Co3 – B8′	2.125(3)
C1 – C2	1.619(4)
B8 – C13	1.684(5)
C1′ – C2′	1.615(4)
Co3-B8-C13	121.1(2)
B4-B8-C13	120.6(3)
B7-B8-C13	130.8(3)

Table 6. Selected bond lengths [Å] and angles [°] for $[\mathrm{Me_4N}][\mathbf{8}]$.

Co3 – C1	2.009(3)
Co3 – C2	1.9901(18)
Co3 – C2′	2.024(2)
Co3 – C1′	2.066(2)
Co3 – B8′	2.160(2)
Co3 – B8	2.170(2)
C1 – C2	1.662(3)
B8-C13	1.652(3)
C1′ – C2′	1.599(3)
Co3-B8-C13	114.37(13)
B4-B8-C13	124.66(18)
B7-B8-C13	121.02(18)

Table 7. Selected bond lengths [Å] and angles [°] for $[\mathrm{Me_4N}][\mathbf{9}]$.

Co3 – C1	2.026(3)
Co3 – C2	2.041(4)
Co3 – C2′	2.051(4)
Co3 – C1′	2.053(3)
Co3 – B8	2.152(4)
Co3 – B8′	2.124(4)
C1 – C2	1.615(5)
B8 – C13	1.599(5)
C1′ – C2′	1.614(4)
Co3-B8-C13	122.6(3)
B4-B8-C13	128.0(3)
B7-B8-C13	124.7(3)

Discussion

Through a B – C coupling reaction it has been possible to cleanly and regioselectively generate monoalkyl and monoaryl derivatives of cobaltabisdicarbollide at the B8 position in good to high yield. Previous to this work, only one of the compounds presented, $[\mathrm{Me_4N}][8\text{-}C_6H_5\text{-}3,3'\text{-}Co(1,2\text{-}C_2B_9H_{10})(1',2'\text{-}C_2B_9H_{11})]$ ($[\mathbf{5}]^-$), had been reported, which was obtained as a by-product and consequently in low yield.[21] The synthetic procedure reported here provides access to a large number of monoalkyl and monoaryl derivatives of $[\mathbf{1}]^-$ and permits systematic study of their electronic properties.

^{11}B chemical shift dependence: Table 1 displays the ^{11}B resonances of $[\mathbf{1}]^- - [\mathbf{9}]^-$. The top row shows the resonances of the parent species $[\mathbf{1}]^-$. As a consequence of the lower symmetry of $[\mathbf{2}]^- - [\mathbf{9}]^-$, the columns become split into two or three, but in such a way that the average of the weighted individual contributions remains very close to the entry in the top row. One clear exception relates to the B – C resonances shown in the first column and the B – I resonance, which is masked by other resonances, in the column with the entry −6.0 in the top row. The constancy of the averaged column values can be interpreted in terms of the perturbation originating from the alkyl or aryl substitution not producing long-range effects, although local effects on the *ipso* boron atom are important, giving rise to a 10 – 13 ppm shift to lower field for alkyl substituents, and a 5 – 7 ppm shift for the aryl analogues. Without exception, the ^{11}B resonance of the B–R moiety (R = alkyl, aryl) is shifted to lower field. If we consider that only the σ_d contribution is relevant in determining the position of the NMR signal, since the chemical shifts of $[\mathbf{1}]^-$ are taken as references, the conclusion would be that the -C(alkyl) groups have a − I influence on boron.[35] The same is true for the local effect created by the -C(aryl) groups,

although for these it is less pronounced. The methyl carbon can only withdraw electron density from the boron, whereas an additional mechanism is available to the aromatic ring, whereby electron density is transferred to a ψ* orbital on the cluster, thereby partly compensating for the loss of local electron density on boron due to the carbon σ bond (see Figure 8). Contrary to the common belief that alkyl groups are electron-releasing, we stress here that they are electron-withdrawing when attached to boron in boron clusters. The following experimental and discussion sections are set out to support this hypothesis.

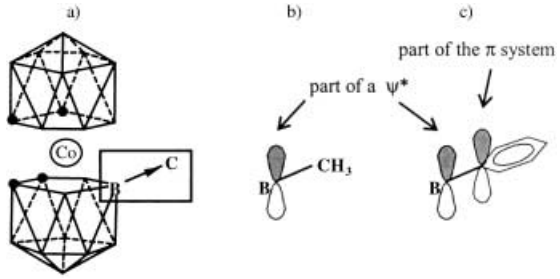

Figure 8. a) Polarization effect of B–C *exo*-cluster bond due to the higher electronegativity of C. When the organic group bonded to the boron atom possesses a double bond (vinyl or aryl group) or a lone pair, a π back-donation to a cluster antibonding ψ* orbital takes place due to orbital overlap as shown in c). This is not possible when the organic group is an alkyl group as in b).

Cyclic voltammetric studies: Only one coupled reduction/oxidation process has been observed for complexes $[\mathbf{1}]^- - [\mathbf{9}]^-$ within the range of potentials studied (-2.5 to -1.0 V, referenced to Fc^+/Fc, which was taken as zero). The reduction current wave is caused by the reduction process "$Co^{III} \rightarrow Co^{II}$";[36] the reverse oxidation process is also observed. Figure 9 shows the cyclic voltammogram of $[\mathbf{9}]^-$ as a

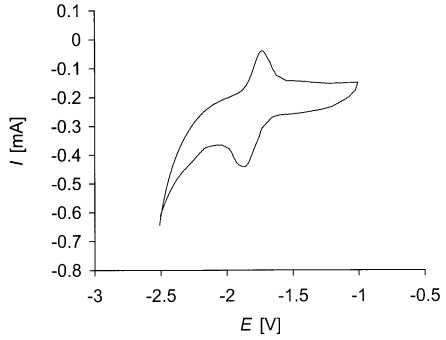

Figure 9. Cyclic voltammogram of compound $[\mathbf{9}]^-$, recorded in acetonitrile containing 0.1 M tetrabutylammonium perchlorate as supporting electrolyte at a scan rate of 100 mV s^{-1}. Potential values are referenced to the Fc^+/Fc couple.

representative example. A conceivable oxidation process beyond the reoxidation of Co^{II} for complexes $[\mathbf{1}]^- - [\mathbf{9}]^-$ was not observed in the range of electrode potentials investigated. Table 8 lists reduction potentials E_{red}, ΔE values ($\Delta E = E_{red} - E_{ox}$), and $E_{1/2}$ ($E_{1/2} = (E_{red} + E_{ox})/2$) for complexes $[\mathbf{1}]^- - [\mathbf{9}]^-$. $E_{1/2}$ is the half-wave potential associated with the Co^{III}/Co^{II} redox process. Among the $E_{1/2}$ values listed, three distinct groupings can be discerned; those of the aryl-substituted derivatives near -1.73 V ($[\mathbf{5}]^-$, $[\mathbf{6}]^-$, $[\mathbf{7}]^-$, $[\mathbf{8}]^-$), those of the non-aryl-substituted derivatives near -1.84 V ($[\mathbf{1}]^-$, $[\mathbf{3}]^-$, $[\mathbf{4}]^-$, $[\mathbf{9}]^-$), and the distinct potential of the iodo derivative ($[\mathbf{2}]^-$) ($E_{1/2} = -1.58$). A simple explanation would be to consider that an electron-releasing substituent R at the π perimeter of the dicarbollide ligand would cause a higher electron density at the Co^{III} center and make it more difficult to reduce, whereas electron-withdrawing groups at the periphery would decrease the reduction overpotential as compared with the parent complex $[\mathbf{1}]^-$. We do not believe that this simple explanation is the right one. It could be satisfactory if $[\mathbf{1}]^-$ was the definitive reference point, with the half-wave potentials $E_{1/2}$ for +I substituents above and those for −I substituents below its potential. However, this is not the case. A more realistic grouping can be made by considering one group of compounds with aromatic substituents ($[\mathbf{5}]^-$, $[\mathbf{6}]^-$, $[\mathbf{7}]^-$, $[\mathbf{8}]^-$) and a second group made up of the alkyl- ($[\mathbf{3}]^-$, $[\mathbf{4}]^-$, $[\mathbf{9}]^-$) and hydrogen-substituted $[\mathbf{1}]^-$. Compound $[\mathbf{2}]^-$ is treated separately. This encouraged us to study the electronic spectra of $[\mathbf{1}]^- - [\mathbf{9}]^-$ and to see if a property existed that differentiated the two sets of compounds. An initial inconvenience that we found was the broadness of the UV/Vis bands, which precluded observation of the individual features of interest.

Table 8. Data obtained from cyclic voltammetry studies in acetonitrile. The $[Fe(C_5H_5)_2]^+/[Fe(C_5H_5)_2]$ couple was taken as the zero reference.

Compound	$E_{1/2}$ [V]	ΔE [V]	E_{red} [V]
$[\mathbf{1}]^-$	−1.83	0.24	−1.95
$[\mathbf{2}]^-$	−1.58	0.27	−1.71
$[\mathbf{3}]^-$	−1.90	0.29	−2.04
$[\mathbf{4}]^-$	−1.81	0.16	−1.89
$[\mathbf{5}]^-$	−1.74	0.23	−1.85
$[\mathbf{6}]^-$	−1.77	0.32	−1.93
$[\mathbf{7}]^-$	−1.67	0.26	−1.83
$[\mathbf{8}]^-$	−1.74	0.21	−1.84
$[\mathbf{9}]^-$	−1.81	0.15	−1.88

UV/Vis spectra: Hawthorne and co-workers[37] have reported that the UV/Vis spectrum of $[\mathbf{1}]^-$ in methanol consists of four absorptions at 216, 293, 345, and 445 nm, which is essentially in agreement with that subsequently reported by Matel and co-workers[25] with one absorption band ($\lambda_{max} = 287$ nm, $\varepsilon \approx 30000$ L cm^{-1} mol^{-1}). The visible spectrum was interpreted by Cerný and co-workers[38] on the basis of ligand field theory.

We have recorded the UV/Vis spectrum of $[\mathbf{1}]^-$ in acetonitrile, as this is the solvent used in the cyclic voltammetry studies, and although the spectrum is rather similar to those already reported, there are some discrepancies in the positions of the maxima and their absorption coefficients, which indicates that these values are strongly dependent on how the absorption (A) is measured. We used the same solvent for all the complexes. The spectra did not show well-defined peaks, which made comparing them difficult; see, for instance, the spectrum of compound **7** shown in Figure 10. To

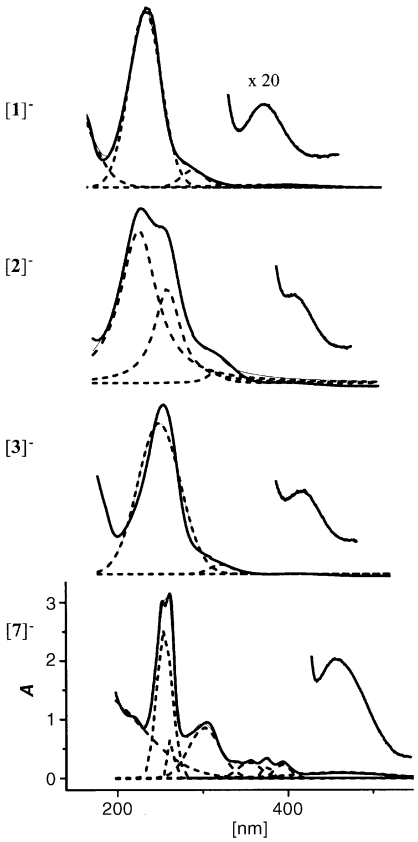

Figure 10. UV/Vis spectra (solid lines) of some selected compounds, from top to bottom $[\mathbf{1}]^-$, $[\mathbf{2}]^-$, $[\mathbf{3}]^-$, and $[\mathbf{7}]^-$, and the results of line fitting with gaussians (dashed lines). The expanded sections on the right show the absorption near 445 nm amplified 20 times.

overcome this problem, a line-fitting analysis was performed.[39] The results obtained are shown in Figure 10 for the parent compound $[\mathbf{1}]^-$, as well as for the B8–I $[\mathbf{2}]^-$, B8–alkyl $[\mathbf{3}]^-$, and B8–aryl $[\mathbf{7}]^-$ derivatives as representative examples. The full set of data is shown in Table 9. As can be seen in Figure 10, the deconvolution with Gaussians permitted discernment of the sub-band positions and the retrieval of λ_{max} and ε data that would otherwise have been impossible. The goodness-of-fit (R^2) of all the spectra was between 0.999 and 0.991. Therefore, relevant comparisons can be made. It can readily be observed that absorptions near 281, 337, and 445 nm, present in the spectrum of $[\mathbf{1}]^-$, are in fact present in all the spectra with comparable ε values. These absorptions are therefore attributed to the $[3,3'\text{-}Co(1,2\text{-}C_2B_9H_{11})_2]^-$ moiety. A second set of absorptions can be ascribed to the aromatic substituents by comparison with the UV/Vis spectrum of the fragment alone; for example, anthracene has two characteristic absorptions at 253 and 375 nm[40] and we observe these bands at 255 and 375 nm in the spectrum of $[\mathbf{7}]^-$. These bands due to the substituents appear at $\lambda < 270$ nm in most of the spectra. Finally, a set of absorptions is observed that cannot be assigned to either of the aforementioned individual fragments, the cluster and the R substituent, and that therefore must be attributed to their interaction. These absorptions appear at around $\lambda = 320$ nm and are only present in the spectra of compounds $[\mathbf{2}]^-$, $[\mathbf{5}]^-$, $[\mathbf{6}]^-$, $[\mathbf{7}]^-$, and $[\mathbf{8}]^-$, and not in those of compounds $[\mathbf{1}]^-$, $[\mathbf{3}]^-$, $[\mathbf{4}]^-$, and $[\mathbf{9}]^-$. Therefore, these absorptions are only found when R contains lone pairs as in $[\mathbf{2}]^-$ or π electrons as in $[\mathbf{5}]^-$, $[\mathbf{6}]^-$, $[\mathbf{7}]^-$, and $[\mathbf{8}]^-$.

The influence of boron: There are similarities and differences between $[Co(C_5H_5)_2]^+$ and compound $[\mathbf{1}]^-$. Both compounds obey the 18 e$^-$ rule, the cobalt is in a +3 oxidation state in both, and 1 e$^-$ reduction should involve the partial filling of the LUMO (see Figure 11). The differences between

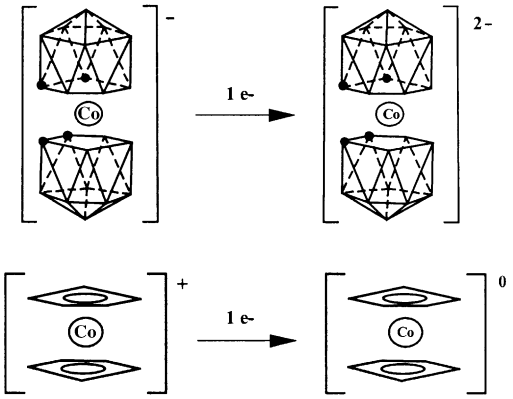

Figure 11. Schematic representations of the 1 e$^-$ reduction processes for compounds $[Co(C_2B_9H_{11})_2]^-$ ($[\mathbf{1}]^-$) and $[Co(C_5H_5)_2]^+$.

$[Co(C_5H_5)_2]^+$ and $[\mathbf{1}]^-$ relate to their charge, their color, and consequently their electronic spectra. While $[Co(C_5H_5)_2]^+$ is yellow-green, $[\mathbf{1}]^-$ is orange. Absorptions in the visible region are found at 404 nm for $[Co(C_5H_5)_2]^+$ and at 445 nm for $[\mathbf{1}]^-$, the former being more energetic than the latter.[38, 41] On the other hand, it is clear that $[C_2B_9H_{11}]^{2-}$ is more effective at

Table 9. UV/Vis spectra for compounds $[\mathbf{1}]^- - [\mathbf{9}]^-$ in acetonitrile. λ positions [nm] and ε values [L cm^{-1} mol^{-1}] are reported and were calculated following line-fitting analysis.

Compound	λ (ε)						
$[\mathbf{1}]^-$	207 (11.698)		281 (27.264)		337 (2.642)		445 (392)
$[\mathbf{2}]^-$			287 (26.604)	320 (9.151)	375 (3.113)		452 (375)
$[\mathbf{3}]^-$			289 (20.943)		362 (2.415)		450 (324)
$[\mathbf{4}]^-$			293 (24.622)		355 (2.075)		450 (313)
$[\mathbf{5}]^-$	223 (13.962)		287 (21.887)	319 (8.207)	366 (3.113)		452 (321)
$[\mathbf{6}]^-$		251 (25.943)*	251 (25.943)*	322 (2.642)	378 (2.075)		450 (377)
$[\mathbf{7}]^-$	214 (9.906)	255 (59.762)	262 (22.381)	320 (2.238)	354 (6.429)	375 (5.000), 393 (5.476)	454 (2.143)
$[\mathbf{8}]^-$	228 (16.981)	272 (10.472)	294 (26.698)	320 (9.340)	379 (3.396)		452 (311)
$[\mathbf{9}]^-$			290 (22.736)		368 (3.132)		452 (371)

stabilizing the highest cobalt oxidation state,[42] Co^{III}, than $[C_5H_5]^-$, and makes its reduction to Co^{II} more difficult. Thus, $E_{1/2}$ values are found at -1.25 V for $[Co(C_5H_5)_2]^+$ and -1.83 V for $[\mathbf{1}]^-$, the second requiring more energy.[43] The mismatch between the electrochemical and visible data led us to think that the redox processes were not parallel in $[Co(C_5H_5)_2]^+$ and $[\mathbf{1}]^-$, suggesting that the participating frontier orbitals did not have the same origin.

The dicarbollide $[C_2B_9H_{11}]^{2-}$ anion has been considered as being isolobal with $[C_5H_5]^-$.[44] Both coordinate in a η^5 manner and produce a rich organometallic chemistry.[16] The main reported differences concern the inward orientation of the open face orbitals in $[C_2B_9H_{11}]^{2-}$, and its capacity to stabilize higher oxidation states. All of the above data led us to think that there are more profound but undetected differences as a consequence of the presence of boron in the coordinating face. Boron is much less electronegative than carbon (2.0 vs 2.5), the difference being the same as that between carbon and nitrogen (2.5 vs 3.0). Consequently, this should differentiate the orbital energies and their capacity to interact with a common metal in the same oxidation state.[8] If a fragment molecular orbital (FMO) analysis is performed on the interactions of $[C_5H_5]^-$ and $[C_2B_9H_{11}]^{2-}$ orbitals with those of a common Co^{III} ion, it is logical to assume that the energy of the HOMO in the ligand fragment should be higher (less negative) in $[C_2B_9H_{11}]^{2-}$ than in $[C_5H_5]^-$, the reason being that there are more boron atoms or comparatively fewer electronegative elements. Therefore, the chances that the HOMO of $[\mathbf{1}]^-$ is, in essence, a Co^{III} d orbital are less than in the case of $[Co(C_5H_5)_2]^+$. At the extreme, the HOMO may not have any contribution from the metal d orbitals. Common thinking is that the HOMO of organometallic complexes is, in essence, a metal d orbital[1] and therefore the $18\,e^-$ rule is mostly obeyed. In a similar way, the LUMO in an organometallic complex is usually thought to be mostly contributed by a metal d orbital. However, this is so because common ligands are invariably made of carbon, or more electronegative elements than carbon. Boron, being to the left of carbon in the Periodic Table, apports fundamental differences.

Influence of the substituents at the cluster B8 position: As stated above, a careful analysis of the line shape in the UV/Vis spectra of $[\mathbf{2}]^-$, $[\mathbf{5}]^-$, $[\mathbf{6}]^-$, $[\mathbf{7}]^-$, and $[\mathbf{8}]^-$ indicated an extra absorption band not attributable to $[\mathbf{1}]^-$ nor to the substituent. This band, near 320 nm, was only observed in the species with direct B8–aryl or B8–I bonds. Interestingly, those compounds having the band near 320 nm ($[\mathbf{2}]^-$, $[\mathbf{5}]^-$–$[\mathbf{8}]^-$) are also those that are more prone to reduction.

To understand the easier reduction of the aryl as compared to the alkyl derivatives of $[\mathbf{1}]^-$, it is necessary to know the origin of the 320 nm band. It is neither due to $[\mathbf{1}]^-$ nor to the aromatic fragment, but to synergy between them. Indeed, this is what is found in the extended Hückel molecular orbital (EHMO) analysis of $[\mathbf{5}]^-$, as shown schematically in Figure 12 for just a few orbitals, including the frontier orbitals. It can clearly be seen that the HOMO is purely due to the cluster fragment, while the LUMO is mostly due to the LUMO+2 of the aromatic fragment, in accord with the UV spectrum and with the notion that the redox processes are not parallel in

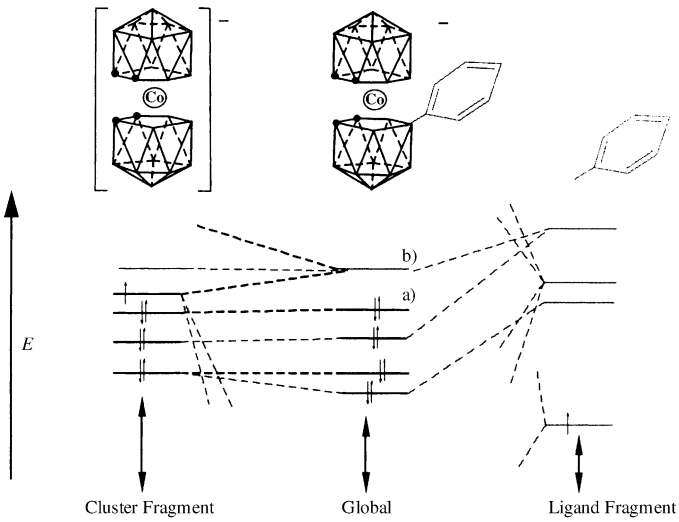

Figure 12. Fragment orbital analysis of $[\mathbf{5}]^-$ showing only relevant frontier orbitals and the contribution of the fragment orbitals. In this approach, the HOMO (a) is purely derived from the cluster fragment and the LUMO (b) contains a significant contribution from orbitals based on the ligand fragment.

$[Co(C_5H_5)_2]^+$ and $[\mathbf{1}]^-$. The $E_{1/2}$ values for the aryl-substituted species can now be nicely interpreted, considering that the HOMO–LUMO gap is diminished in the aryl-substituted compounds as compared to that in $[\mathbf{1}]^-$, thus requiring a less cathodic potential for the reduction to proceed.

On incorporation of boron into the coordinating carbocycle, that is, on going from $[C_5H_5]^-$ to the C_2B_3 open face in $[C_2B_9H_{11}]^{2-}$, there is a greater energy mismatch between the relevant orbitals on the ligand and on the metal that generate the frontier orbital in the complex, the net effect of which is that the orbital overlap is no longer very efficient. The participation of the metal orbitals in the molecular frontier orbitals is less, or, in other words, the contribution from the ligand orbitals in the frontier orbitals is larger. Therefore, besides the influence of the central metal ion on the energy of the molecular orbitals, it seems clear that the relative contribution from the boron-containing ligands in the more relevant frontier orbital features is large, contrary to what is assumed for conventional η^5 ligands.

Comparison of the structures of $[\mathbf{3}]^-$ and $[\mathbf{5}]^-$ offers relevant information concerning the participation of the metal d orbitals in frontier orbitals. Wagner and co-workers[45] studied the α^* dip angle, defined as the angle between the center of gravity of the substituted cyclopentadienyl ring, the *ipso* carbon atom, and the exocyclic carbon atom (or boron), in order to measure the degree of substituent bending in ferrocenyl carbocations and borylferrocene. The larger the value of α^*, the greater the interaction between the filled d-type orbitals at the metal and the empty p orbital at boron (or carbon). The same strategy can also be used to assess the possibility of interaction between cobalt d orbitals and the π aromatic system in the compounds described herein, for instance in $[\mathbf{5}]^-$. Wagner reported α^* values of about 18° in $[Fe(C_5H_5)(BR_2\text{-}C_5H_4)]$. In conventional metallocenes, the reference point is practically zero. However, substituents on $[7,8\text{-}C_2B_9H_{11}]^{2-}$ derivatives already present a natural dip angle

and therefore in sandwich metallaboranes it is necessary to base discussion on $\Delta\alpha^*$, the reference value being provided by the experimental α^* value found for $[\mathbf{3}]^-$, which is 16.3°. The value of α^* for $[\mathbf{5}]^-$ is 20.7°, and thus $\Delta\alpha^*$ is 4.4°, which suggests that there is a degree of interaction, albeit minor, between the d orbitals on the metal and orbitals of suitable symmetry on the aryl moiety.

ab initio Interpretation: All the above interpretations based on experimental observations are supported by ab initio calculations[46] on $[\mathbf{1}]^-$, $[\mathbf{2}]^-$, $[\mathbf{3}]^-$, $[\mathbf{5}]^-$, $[\mathbf{8}]^-$, and $[\mathbf{9}]^-$. Calculations have been performed on these because geometrical parameters are either presented in this paper ($[\mathbf{3}]^-$, $[\mathbf{8}]^-$, and $[\mathbf{9}]^-$) or are available elsewhere ($[\mathbf{1}]^-$,[47] $[\mathbf{5}]^-$,[21] and $[\mathbf{2}]^-$[48]). A single-point calculation at the HF/3-21 G level was performed on all of them, with the exception of $[\mathbf{2}]^-$, in the case of which all atoms were computed with the 3-21 G basis set but the iodine was computed at 6 G*. To reduce computational time, the butyl group in $[\mathbf{8}]^-$ was converted into an ethyl group by simply replacing the terminal -CH_2CH_3 moiety by a hydrogen. The new C–H distance was set at the average of the two remaining C–H lengths. No other approximations were made. Table 10 displays the HOMO and LUMO energies, the LUMO and HOMO energy gap, and the $E_{1/2}$ potential value, as also reported in Table 8. The compounds are ordered with respect to their reduction potentials. Compound $[\mathbf{3}]^-$ is the most difficult to reduce and compound $[\mathbf{2}]^-$ is the most easily reducible. Interestingly, the $E_{1/2}$ column fully parallels the HOMO energy column. This was, in principle, unexpected as, according to Koopman's theorem, this property would be related to the $Co^{III} \rightarrow Co^{IV}$ process. A good matching with the LUMO–HOMO gap column related to the $Co^{III} \rightarrow Co^{II}$ process was also found. The only discrepancies are found for $[\mathbf{9}]^-$ and $[\mathbf{5}]^-$, which have practically identical LUMO–HOMO values but a 70 mV difference in $\Delta E_{1/2}$. It is possible that a larger basis set would account for these differences.

Table 10. Relationship of frontier orbitals energy and redox potential.

Compound	E_{HOMO}	E_{LUMO}	$\Delta E_{(HOMO\text{-}LUMO)}$	$E_{1/2}$ [V]
$[\mathbf{3}]^-$	– 6.46939	5.283453	– 11.752843	– 1.90
$[\mathbf{1}]^-$	– 6.246414	5.453047	– 11.699461	– 1.83
$[\mathbf{9}]^-$	– 6.14250	5.136343	– 11.278843	– 1.81
$[\mathbf{5}]^-$	– 5.727132	5.563548	– 11.29068	– 1.74
$[\mathbf{8}]^-$	– 5.550179	5.47337	– 11.023549	– 1.74
$[\mathbf{2}]^-$	– 5.479989	5.503018	– 10.983007	– 1.58

Looking at the spatial disposition of the HOMO and LUMO for $[\mathbf{2}]^-$, $[\mathbf{5}]^-$, and $[\mathbf{8}]^-$, it is clear that the HOMO is centered on the lone pair or π electron containing substituent (I, Ph) and that the LUMO is a metal d orbital (see Figure 13 for a representation of the HOMO and LUMO for $[\mathbf{5}]^-$). Therefore, the LUMO–HOMO gap is the result of the combined effect of the two molecular fragments, as evidenced experimentally by UV/Vis spectroscopy and studied by line-fitting analysis. Inspection of the spatial disposition of the orbitals also reveals that the frontier orbitals are not the same

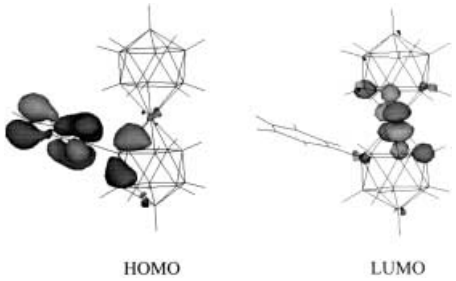

Figure 13. Representation of the HOMO and LUMO for $[\mathbf{5}]^-$.

in the two sets of compounds. For $[\mathbf{1}]^-$, $[\mathbf{3}]^-$, and $[\mathbf{9}]^-$, the LUMOs have the same origin, but it is not a d orbital; the d orbitals mostly participate in LUMO+1 and LUMO+2. On the contrary, the HOMOs are different, a d orbital in $[\mathbf{1}]^-$, a cluster spread molecular orbital in $[\mathbf{3}]^-$, and a π orbital on the phenyl fragment in $[\mathbf{9}]^-$.

We have differentiated two sets of compounds through the presence or absence of an aromatic ring. Nevertheless, it is possible that the sequential energy destabilization of the HOMO shown in Table 10 on going from the alkyl through the aryl $[3,3'\text{-}Co(1,2\text{-}C_2B_9H_{11})_2]^-$ derivatives to the iodo derivative may be related to the $-I$ character of the methyl group when bonded to boron. One electronegative element causes a greater stabilization of one filled orbital. According to Table 10, the HOMO of $[\mathbf{3}]^-$ is the most stabilized, while that of $[\mathbf{2}]^-$ is the most destabilized. All else being equal, this supports our concept of a –I methyl group. The effect of the phenyl group, although very similar, is mitigated by electron back-donation to the boron. The case of the iodo derivative ($[\mathbf{2}]^-$) can easily be explained considering that iodine has an Allred–Rochow electronegativity of 2.2 compared to 2.5 for carbon and that the back-donation effect is large due to the high polarizability of the iodine lone pairs.

Conclusion

Regioselective monoalkylation and monoarylation in cobaltabisdicarbollide clusters has been successfully accomplished by cross-coupling reactions between a B–I fragment and an appropriate Grignard reagent in the presence of a Pd catalyst and CuI. This has facilitated the preparation of a considerable number of monoalkylated and monoarylated derivatives, which, in turn, has permitted study of the influence of boron in metallocene-type ligands and the effect of alkyl and aryl substituents on boron in boron anionic clusters. Experimental data from UV/Vis spectroscopy, $E_{1/2}$ measurements, and X-ray diffraction analysis, and supported by EHMO and ab initio analyses, indicate that the participation of metal d orbitals in the HOMOs of these complexes is less than that in typical metallocene complexes. This can be explained as a consequence of the lower electronegativity of boron as compared to carbon. Related to this is the –I character of alkyl groups when bonded to boron in boron anionic clusters, contrary to the common belief that alkyl groups are generally electron-donating groups. Alkyl groups are donating towards elements of equal or greater electronegativity, but boron is less

electronegative. Relevant to this discussion is the accepted negative character of the methyl group in MeLi as a result of $\chi_{Li} = 1.0$ and $\chi_C = 2.5$.

Experimental Section

General considerations: Elemental analyses were performed using a Carlo Erba EA 1108 microanalyzer. IR spectra were recorded from samples in KBr pellets on a Shimadzu FTIR-8300 spectrophotometer. UV/Vis spectroscopy was carried out with a Cary 5E spectrophotometer using 0.1 cm cuvettes. The concentration of the complexes was 1×10^{-3} mol L^{-1}. ^{1}H and ^{1}H{^{11}B} NMR (300.13 MHz), ^{13}C{^{1}H} NMR (75.47 MHz), and ^{11}B NMR (96.29 MHz) spectra were recorded with a Bruker ARX 300 instrument equipped with the appropriate decoupling accessories. Chemical shift values for ^{11}B NMR spectra are referenced to external $BF_3 \cdot OEt_2$, and those for ^{1}H, ^{1}H{^{11}B}, and ^{13}C{^{1}H} NMR spectra are referenced to $SiMe_4$. Chemical shifts are reported in units of parts per million downfield from the reference signal, and all coupling constants are reported in Hertz.

Unless otherwise noted, all manipulations were carried out under a dinitrogen atmosphere using standard vacuum line techniques. THF was distilled from sodium/benzophenone prior to use. EtOH was dried over molecular sieves and deoxygenated prior to use. The cesium salt of compound [**1**]$^-$ was supplied by Katchem Ltd. (Prague) and was used as received. All other reagents were obtained commercially and were used as purchased. Bis(triphenylphosphine)palladium dichloride[49] was synthesized according to the literature.

Electrochemical measurements were performed in a standard double-compartment three-electrode cell. Ag/AgCl/[nBu$_4$N]Cl (0.1 M in MeCN) was used as a reference electrode. A 4 mm^2 platinum plate and a platinum wire were used as working and counter electrode, respectively. All measurements were performed in acetonitrile with 0.1 M tetrabutylammonium perchlorate as supporting electrolyte. Cyclic voltammograms were recorded at a scan rate of 100 mV s^{-1}. The mass spectra were recorded in negative-ion mode using a Bruker Biflex MALDI-TOF MS [N_2 laser; λ_{exc} 337 nm (0.5 ns pulses); voltage ion source 20.00 kV (Uis 1) and 17.50 kV (Uis 2)].

Synthesis of Cs[8-I-3,3′-Co(1,2-C$_2$B$_9$H$_{10}$)(1′,2′-C$_2$B$_9$H$_{11}$)] (Cs[2]): Iodine (1.67 g, 6.58 mmol) was added to a solution of Cs[**1**] (1.5 g, 3.28 mmol) in EtOH (20 mL). The reaction mixture was left to stand overnight at room temperature and was then heated under reflux for 2.5 h. The excess iodine was decomposed by the addition of a solution of Na_2SO_3 (0.66 g, 5.26 mmol) in water (16 mL) and the resulting mixture was boiled for 5 min. The mixture was concentrated until the precipitation of an orange solid. This was filtered off, washed with water and petroleum ether, and dried in vacuo (1.82 g, 95 %). ^{1}H{^{11}B} NMR (300 MHz, [D$_6$]acetone, 25 °C, TMS): $\delta = 4.54$ (brs, 2H; C$_c$–H), 4.29 (brs, 2H; C$_c$–H), 3.04 (brs, 2H; B–H), 2.59 (brs, 2H; B–H), 2.46 (brs, 4H; B–H), 1.93 (brs, 4H; B–H), 1.84 (brs, 1H; B–H), 1.77 (brs, 2H; B–H), 1.70 (brs, 2H; B–H); IR (KBr): $\tilde{\nu} =$ 3040, 3032 (C$_c$–H), 2574, 2542, 2500 (B–H), 1138, 1099, 1016, 976, 617, 773, 750 cm^{-1}; MALDI-TOF MS: m/z (%): 449.3 (100) [M^+], 323.5 (47) [$M^+ -$ I]; elemental analysis calcd (%) for C$_4$H$_{21}$B$_{18}$CoCsI: C 8.25, H 3.63; found: C 8.35, H 3.50.

Synthesis of [nBu$_4$N][8-Me-3,3′-Co(1,2-C$_2$B$_9$H$_{10}$)(1′,2′-C$_2$B$_9$H$_{11}$)] ([nBu$_4$N][3]): A solution of Cs[**2**] (1.0 g, 1.72 mmol) in THF (100 mL) was treated with methylmagnesium bromide (2.29 mL, 3.0 M in diethyl ether; 6.88 mmol) at −84 °C, forming a brown precipitate. The mixture was allowed to warm to room temperature, and then [PdCl$_2$(PPh$_3$)$_2$] (0.14 g, 0.21 mmol) and CuI (0.049 g, 0.26 mmol) were added. The mixture was refluxed for 20 h. Twenty drops of water were then added to quench the excess Grignard reagent, and the solvent was removed in vacuo. The residue was extracted with dichloromethane (3 × 30 mL) and the remaining black insoluble material was discarded. The solvent was removed and water (30 mL) was added to the yellow residue. This was extracted with diethyl ether (3 × 30 mL), and the combined organic layers were dried over anhydrous magnesium sulfate. The solvent was removed, the product was redissolved in hot water (50 mL), and [nBu$_4$N]Cl · H$_2$O (0.96 g, 3.44 mmol) was added to precipitate the product. The precipitate was collected by filtration and dried in vacuo (0.91 g, 91 %). ^{1}H{^{11}B} NMR (300 MHz, [D$_6$]acetone, 25 °C, TMS): $\delta = 4.08$ (brs, 2H; C$_c$–H), 3.87 (brs, 2H; C$_c$–H), 3.44 (t, ^3J(H,H) = 8 Hz, 8H; N(CH$_2$CH$_2$CH$_2$CH$_3$)$_4$), 2.93 (brs, 2H; B–H), 2.73 (brs, 2H; B–H), 2.65 (brs; B–H), 1.96 (brs; B–H), 1.91 (brs; B–H), 1.68 (brs; B–H), 1.79 (q, ^3J(H,H) = 8 Hz, 8H; N(CH$_2$CH$_2$CH$_2$CH$_3$)$_4$), 1.58 (brs; B–H), 1.42 (h, ^3J(H,H) = 7 Hz, 8H; N(CH$_2$CH$_2$CH$_2$CH$_3$)$_4$), 0.98 (t, ^3J(H,H) = 7 Hz, 12H; N(CH$_2$CH$_2$CH$_2$CH$_3$)$_4$), 0.59 (brs, 3H; B–Me); IR (KBr): $\tilde{\nu} =$ 3055 (C$_c$–H), 2962, 2922, 2873 (C$_{alkyl}$–H), 2554 (B–H), 1465, 1436, 1383 (δ(C–H)$_{alkyl}$), 1100, 1098 (B–C), 973 (υ_{as}(C–N)), 718, 694 (γ(C–H)), 535 cm^{-1}; MALDI-TOF MS: m/z (%): 338.6 (100) [M^+]; elemental analysis calcd (%) for C$_{21}$H$_{60}$B$_{18}$CoN: C 43.47, H 10.42, N 2.41; found: C 43.15, H 10.50, N 2.57.

Synthesis of [Me$_4$N][8-Et-3,3′-Co(1,2-C$_2$B$_9$H$_{10}$)(1′,2′-C$_2$B$_9$H$_{11}$)] ([Me$_4$N][4]): A solution of ethylmagnesium bromide (3.0 M in diethyl ether; 0.46 mL, 1.37 mmol) was added dropwise to a stirred solution of Cs[**2**] (200 mg, 0.34 mmol) in THF (50 mL) at 0 °C. The mixture was set aside at room temperature for 2 h and then [PdCl$_2$(PPh$_3$)$_2$] (10 mg, 0.01 mmol) and CuI (2 mg, 0.01 mmol) were added in a single portion. The brown solution was refluxed for 20 min and a grey solid was filtered off and discarded. After removal of the solvent, diethyl ether (20 mL) was added to the residue and the excess Grignard reagent was destroyed by the slow addition of dilute HCl. The organic phase was separated, and the aqueous layer was extracted with diethyl ether (3 × 20 mL). The combined organic layers were washed with water (3 × 20 mL) and dried over anhydrous magnesium sulfate. The solvent was removed. The residue was dissolved in the minimum volume of EtOH and an aqueous solution containing an excess of [Me$_4$N]Cl was added, resulting in the formation of a precipitate. This was filtered off, washed with water and petroleum ether, and dried in vacuo (117 mg, 80 %). ^{1}H{^{11}B} NMR (300 MHz, [D$_6$]acetone, 25 °C, TMS): $\delta = 4.10$ (brs, 2H; C$_c$–H), 3.88 (brs, 2H; C$_c$–H), 3.42 (s, 12H; Me$_4$N), 3.06 (brs, 2H; B–H), 2.90 (brs, 2H; B–H), 2.71 (brs, 2H; B–H), 2.64 (brs, 1H; B–H), 1.94 (brs, 2H; B–H), 1.86 (brs, 2H; B–H), 1.64 (brs, 2H; B–H), 1.57 (brs, 4H; B–H), 1.18 (q, ^3J(H,H) = 8 Hz, 2H; CH_2CH$_3$), 0.87 (t, ^3J(H,H) = 8 Hz, 3H; CH$_2$CH_3); IR (KBr): $\tilde{\nu} =$ 3038 (C$_c$–H), 2941, 2922, 2862 (C$_{alkyl}$–H), 2544, 2513 (B–H), 1481 (δ(C–H)$_{alkyl}$), 947 (υ_{as}(C–N)), 743, 719 cm^{-1} (B–C); MALDI-TOF MS: m/z (%): 352.5 (100) [M^+]; elemental analysis calcd (%) for C$_{10}$H$_{38}$B$_{18}$CoN: C 28.20, H 8.99, N 3.29; found: C 28.18, H 9.05, N 3.27.

Synthesis of [Me$_4$N][8-C$_6$H$_5$-3,3′-Co(1,2-C$_2$B$_9$H$_{10}$)(1′,2′-C$_2$B$_9$H$_{11}$)] ([Me$_4$N][5]): Similarly, Cs[**2**] (200 mg, 0.34 mmol) in THF (50 mL) and a solution of phenylmagnesium bromide (1.0 mL; 1.37 mmol), prepared from magnesium turnings (0.67 g, 27.56 mmol) and bromobenzene (1.5 mL, 14.27 mmol), were reacted at 0 °C in THF (10 mL). After 30 min at room temperature, [PdCl$_2$(PPh$_3$)$_2$] (10 mg, 0.01 mmol) and CuI (2 mg, 0.01 mmol) were added. The brown solution was heated under reflux for 2 h. Work-up and purification as described above gave [Me$_4$N][**5**] (150 mg, 92 %). ^{1}H{^{11}B} NMR (300 MHz, [D$_6$]acetone, 25 °C, TMS): $\delta = 7.32 - 7.01$ (m, 5H; C$_6$H$_5$), 4.58 (brs, 2H; C$_c$–H), 3.76 (brs, 2H; C$_c$–H), 3.42 (s, 12H; Me$_4$N), 3.12 (brs, 2H; B–H), 2.91 (brs, 2H; B–H), 2.85 (brs, 4H; B–H), 2.77 (brs, 2H; B–H), 1.93 (brs, 2H; B–H), 1.79 (brs, 4H; B–H), 1.75 (brs, 1H; B–H); IR (KBr): $\tilde{\nu} =$ 3028 (C$_c$–H), 2961, 2874 (C$_{aryl/alkyl}$–H), 2554, 2536, 2473 (B–H), 1479 (δ(C–H)$_{alkyl}$), 947 (υ_{as}(C–N)), 742, 704 cm^{-1} (B–C); MALDI-TOF MS: m/z (%): 400.8 (100) [M^+]; elemental analysis calcd (%) for C$_{14}$H$_{38}$B$_{18}$CoN: C 35.48, H 8.08, N 2.96; found: C 35.30, H 8.00, N 2.93.

Synthesis of [Me$_4$N][8-C$_{12}$H$_9$-3,3′-Co(1,2-C$_2$B$_9$H$_{10}$)(1′,2′-C$_2$B$_9$H$_{11}$)] ([Me$_4$N][6]): Similarly, Cs[**2**] (200 mg, 0.34 mmol) in THF (50 mL) and a solution of biphenylmagnesium bromide (1.37 mmol), prepared from magnesium turnings (67 mg, 2.75 mmol) and 4-bromobiphenyl (0.32 g, 1.37 mmol), were reacted at 0 °C in THF (6.0 mL). After 30 min at room temperature, [PdCl$_2$(PPh$_3$)$_2$] (10 mg, 0.01 mmol) and CuI (2 mg, 0.01 mmol) were added. The brown solution was refluxed for 2 d. Work-up and purification as described above gave [Me$_4$N][**6**] (180 mg, 95 %). ^{1}H{^{11}B} NMR (300 MHz, [D$_6$]acetone, 25 °C, TMS): $\delta = 7.66 - 7.35$ (m, 5H; C$_{12}$H$_9$), 4.60 (brs, 2H; C$_c$–H), 3.87 (brs, 2H; C$_c$–H), 3.36 (s, 12H; Me$_4$N), 3.18 (brs, 2H; B–H), 2.95 (brs, 1H; B–H), 2.82 (brs, 2H; B–H), 2.63 (brs, 1H; B–H), 2.18 (brs, 1H; B–H), 2.04 (brs, 4H; B–H), 1.77 (brs, 4H; B–H), 1.53 (brs, 2H; B–H); IR (KBr): $\tilde{\nu} =$ 3028 (C$_c$–H), 2961, 2922, 2866 (C$_{aryl/alkyl}$–H), 2559 (B–H), 1481 (δ(C–H)$_{alkyl}$), 945 (υ_{as}(C–N)), 740, 700 cm^{-1} (B–C); MALDI-TOF MS: m/z (%): 476.6 (100) [M^+]; elemental analysis calcd (%) for C$_{20}$H$_{42}$B$_{18}$CoN: C 43.67, H 7.70, N 2.55; found: C 43.50, H 7.60, N 2.50.

Synthesis of Cs[8-$C_{14}H_9$-3,3′-Co(1,2-$C_2B_9H_{10}$)(1′,2′-$C_2B_9H_{11}$)] (Cs[7]): Similarly, Cs[**2**] (100 mg, 0.17 mmol) in THF (25 mL) was treated with a solution of anthracenylmagnesium bromide (1.37 mmol), prepared from magnesium turnings (67 mg, 2.75 mmol) and 9-bromoanthracene (0.35 g, 1.37 mmol) in THF (24 mL) at 0 °C. After 30 min at room temperature, [$PdCl_2(PPh_3)_2$] (10 mg, 0.01 mmol) and CuI (2 mg, 0.01 mmol) were added. The brown solution was heated under reflux for 41 h. Some drops of water were added to destroy the excess Grignard reagent and the solid was filtered off and discarded. The solution was concentrated, causing the precipitation of a red solid, which was collected by filtration and dried in vacuo (83 mg, 76 %). $^1H\{^{11}B\}$ NMR (300 MHz, [D_6]acetone, 25 °C, TMS): $\delta = 9.40$, 8.53, 8.24, 8.05, 7.88, 7.51, 7.32, 6.95 (m, 9H; $C_{14}H_9$), 4.52 (brs, 2H; C_c–H), 3.82 (brs, 4H; B–H), 3.15 (brs, 1H; B–H), 3.08 (brs, 2H; C_c–H), 2.71 (brs, 2H; B–H), 2.63 (brs, 2H; B–H), 2.58 (brs, 2H; B–H), 1.95 (brs, 1H; B–H), 1.58 (brs, 2H; B–H), 1.11 (brs, 2H; B–H), 0.71 (brs, 1H; B–H); IR (KBr): $\tilde{\nu} = 3047$ (C_c–H), 2970 (C_{aryl}–H), 2559 (B–H), 727 cm^{-1} (B–C); MALDI-TOF MS: *m*/*z* (%): 501.7 (100) [M^+]; elemental analysis calcd (%) for $C_{18}H_{30}B_{18}CoCs$: C 34.16, H 4.78; found: C 34.26, H 4.80.

Synthesis of [Me_4N][8-C_6H_4*n*Bu-3,3′-Co(1,2-$C_2B_9H_{10}$)(1′,2′-$C_2B_9H_{11}$)] ([Me_4N][8]): Similarly, Cs[**2**] (200 mg, 0.34 mmol) in THF (40 mL) was treated with a solution of 4-butylphenylmagnesium bromide (1.37 mmol), prepared from magnesium turnings (67 mg, 2.75 mmol) and 1-bromo-4-butylbenzene (0.24 mL, 1.37 mmol) in THF (6 mL) at 0 °C. After 30 min at room temperature, [$PdCl_2(PPh_3)_2$] (96 mg, 0.04 mmol) and CuI (26 mg, 0.04 mmol) were added. The reaction mixture was refluxed for 5 min and was left at room temperature overnight. Work-up and purification as described above gave [Me_4N][**8**] (170 mg, 93 %). $^1H\{^{11}B\}$ NMR (300 MHz, [D_6]acetone, 25 °C, TMS): $\delta = 7.21$ (d, $^3J(H,H) = 8$, 2H, C_6H_4), 6.92 (d, $^3J(H,H) = 8$, 2H, C_6H_4), 4.60 (brs, 2H, C_c–H), 3.73 (brs, 2H, C_c–H), 3.42 (s, 12H, Me_4N), 3.11 (brs, 2H, B–H), 2.86 (brs, 2H, B–H), 2.80 (brs, 2H, B–H), 2.50 (t, $^3J(H,H) = 8$, 2H, $CH_2CH_2CH_2CH_3$), 1.92 (brs, 2H, B–H), 1.74 (brs, 2H, B–H), 1.71 (brs, 2H, B–H), 1.54 (c, $^3J(H,H) = 8$, 2H, $CH_2CH_2CH_2CH_3$), 1.50 (brs, 3H, B–H), 1.41 (brs, 2H, B–H), 1.30 (h, $^3J(H,H) = 7$, 2H, $CH_2CH_2CH_2CH_3$), 0.89 (t, $^3J(H,H) = 7$, 2H, $CH_2CH_2CH_2CH_3$); IR (KBr): $\tilde{\nu} = 3038$ ($C_{cluster/aryl}$–H), 2951, 2928, 2856 (C_{alkyl}–H), 2534 (B–H), 1479 (δ(C–H)$_{alkyl}$), 947 (υ_{as}(C–N)), 742, 702 cm^{-1} (B–C); elemental analysis calcd (%) for $C_{18}H_{46}B_{18}CoN$: C 40.78, H 8.75, N 2.64; found: C 40.69, H 8.68, N 2.67.

Synthesis of [Me_4N][8-$C_2H_4C_6H_5$-3,3′-Co(1,2-$C_2B_9H_{10}$)(1′,2′-$C_2B_9H_{11}$)] ([Me_4N][9]): Similarly, Cs[**2**] (200 mg, 0.34 mmol) in THF (15 mL) was treated with a solution of 2-phenylethylmagnesium bromide (1.37 mmol), prepared from magnesium turnings (67 mg, 2.75 mmol) and (2-bromoethyl)benzene (0.19 mL, 1.37 mmol) in THF (6 mL) at 0 °C. After 30 min at room temperature, [$PdCl_2(PPh_3)_2$] (96 mg, 0.04 mmol) and CuI (26 mg, 0.04 mmol) were added. The reaction mixture was refluxed for 15 min and was left at room temperature overnight. Work-up and purification as described above gave [Me_4N][**9**] (140 mg, 81 %). $^1H\{^{11}B\}$ NMR (300 MHz, [D_6]acetone, 25 °C, TMS): $\delta = 7.18$ (m(a), C_6H_5), 4.12 (brs, 2H, C_c–H), 3.92 (brs, 2H, C_c–H), 3.37 (s, 12H, Me_4N), 2.95 (brs, 2H, B–H), 2.82 (brs, 2H, B–H), 2.72 (brs, 2H, B–H), 2.08 (t, $^3J(H,H) = 3$, 2H, CH_2), 1.91 (brs, 3H, B–H), 1.60 (brs, 8H, B–H), 1.40 (t, $^3J(H,H) = 3$, 2H, CH_2); IR (KBr): $\tilde{\nu} =$ 3028 ($C_{cluster/aryl}$–H), 2922, 2854 (C_{alkyl}–H), 2602, 2554, 2523 (B–H), 1479 (δ(C–H)$_{alkyl}$), 943 (υ_{as}(C–N)), 762, 706 cm^{-1} (B–C); elemental analysis calcd (%) for $C_{16}H_{42}B_{18}CoN$: C 38.28, H 8.43, N 2.79; found: C 37.98, H 8.33, N 2.82.

X-ray crystallography: Single-crystal data collections for [nBu$_4$N][**3**], [Me_4N][**8**], and [Me_4N][**9**] were performed at −100 °C on an Enraf-Nonius KappaCCD diffractometer using graphite-monochromated $Mo_{K\alpha}$ radiation. A total of 6075, 4403, and 5083 unique reflections were collected for [nBu$_4$N][**3**], [Me_4N][**8**], and [Me_4N][**9**], respectively. The structures were solved by direct methods and refined against F^2 using the SHELXL97 program.[50] For all structures, the hydrogen atoms were treated as riding using the SHELXL97 default parameters. For [nBu$_4$N][**3**], all non-hydrogen atoms were refined with anisotropic displacement parameters.

In the case of [Me_4N][**8**], for the butyl chain connected to the phenyl group only the vicinal carbon atom of the latter could be clearly located in the Fourier map. In the vicinity of this carbon, a bulky volume with an electron density of just below 1.0 e Å^{-3} was found, indicating that neither of the other three carbon atoms of the butyl chain occupies a defined position, and that the chain does not have a fixed orientation in the solid state. Possible positions of the three "missing" atoms of the butyl chain were assumed and the chain was refined by applying DFIX restraints and a fixed isotropic thermal displacement parameter of 0.2 Å^{-2} for the three terminal carbon atoms. The $[Me_4N]^+$ ion is disordered with the central nitrogen occupying one position but each of the methyl groups split between two positions. The disordered methyl carbons of the $[Me_4N]^+$ ion and the three terminal carbon atoms of the butyl chain were refined with isotropic displacement parameters, but the remaining non-hydrogen atoms were refined with anisotropic displacement parameters. [Me_4N][**8**] crystallizes in a non-centrosymmetric space group, and its absolute configuration was determined by refinement of the Flack *x* parameter. [Me_4N][**8**] has a lot of pseudo symmetry, as a result of which it can also be refined in the centrosymmetric space group *C*2/*c*, but this results in higher *R* values and a chemically unrealistic 1D structure.

For [Me_4N][**9**], the $[Me_4N]^+$ ion is disordered showing rotational disorder about the N–C21 bond. The three disordered carbon atoms of the $[Me_4N]^+$ ion were refined with isotropic displacement parameters, but the remaining non-hydrogen atoms were refined with anisotropic displacement parameters. [Me_4N][**9**] crystallizes in a non-centrosymmetric space group, and its absolute configuration was determined by refinement of the Flack *x* parameter.

CCDC-206027, -206028, and -206029, [nBu$_4$N][8-Me-3,3′-Co(1,2-$C_2B_9H_{10}$)(1′,2′-$C_2B_9H_{11}$)], ([nBu$_4$N][**3**]), [Me_4N][8-C_6H_4*n*Bu-3,3′-Co(1,2-$C_2B_9H_{10}$)(1′,2′-$C_2B_9H_{11}$)], ([Me_4N][**8**]), and [Me_4N][8-$C_2H_4C_6H_5$-3,3′-Co(1,2-$C_2B_9H_{10}$)(1′,2′-$C_2B_9H_{11}$)], ([Me_4N][**9**]) contain the supplementary crystallographic data for this paper. These data can be obtained free of charge via www.ccdc.cam.ac.uk/conts/retrieving.html (or from the Cambridge Crystallographic Data Centre, 12 Union Road, Cambridge CB2 1EZ, UK; fax: (+44) 1223-336033; or deposit@ccdc.cam.uk).

Acknowledgement

We thank ENRESA for partial support of this research, as well as MCyT (MAT01–1575) and the Generalitat de Catalunya 2001/SGR/00337.

[1] a) N. J. Long, *Metallocenes: An Introduction to Sandwich Complexes*, Blackwell Science, **1998**; b) A. Togni, R. L. Halterman, *Metallocenes: Synthesis-Reactivity-Applications*, Wiley-VCH, New York, **1998**.
[2] a) J. Ebels, R. Pietschnig, S. Kotila, A. Dombrowski, E. Niecke, M. Nieger, H. M. Schiffner, *Eur. J. Inorg. Chem.* **1998**, 331; b) P. Jutzi, *Comm. Inorg. Chem.* **1987**, *6*, 123.
[3] M. M. Conejo, R. Fernández, E. Gutiérrez-Puebla, A. Monge, C. Ruiz, E. Carmona, *Angew. Chem.* **2000**, *112*, 2025; *Angew. Chem. Int. Ed.* **2000**, *39*, 1949.
[4] G. Rossetto, P. Zanella, G. Carta, R. Bertani, D. Favretto, G. M. Ingo, *Appl. Organomet. Chem.* **1999**, *13*, 509.
[5] D. Zargarian, *Coord. Chem. Rev.* **2002**, 102, 157.
[6] a) N. Kuhn, *Bull. Soc. Chim. Belg.* **1990**, *99*, 707; b) N. Kuhn, G. Henkel, S. Stubenrauch, *Angew. Chem.* **1992**, *104*, 766; *Angew. Chem. Int. Ed. Engl.* **1992**, *31*, 778; c) N. Kuhn, M. Köckerling, S. Stubenrauch, D. Bläser, R. Boese, *J. Chem. Soc. Chem. Commun.* **1991**, 1368.
[7] a) C. Janiak, N. Kuhn, R. Gleiter, *J. Organomet. Chem.* **1994**, *475*, 223; b) N. Kuhn, G. Henkel, J. Kreutzberg, S. Stubenrauch, C. Janiak, *J. Organomet. Chem.* **1993**, *456*, 97.
[8] T. A. Albright, J. K. Burdett, M. H. Whangbo, *Orbital Interactions in Chemistry*, Wiley-Interscience, New York, **1985**, pp. 219.
[9] T. Peymann, C. B. Knobler, M. F. Hawthorne, *J. Am. Chem. Soc.* **1999**, *121*, 5601.
[10] a) B. T. King, Z. Janousek, B. Grüner, M. Trammell, B. C. Noll, J. Michl, *J. Am. Chem. Soc.* **1996**, *118*, 3313; b) D. Stasko, C. A. Reed, *J. Am. Chem. Soc.* **2002**, *124*, 1148; c) M. J. Ingleson, M. F. Mahon, N. J. Patmore, G. D. Ruggiero, A. S. Weller, *Angew. Chem.* **2002**, *114*, 3846; *Angew. Chem. Int. Ed.* **2002**, *41*, 3694.
[11] W. Jiang, C. B. Knobler, M. D. Mortimer, M. F. Hawthorne, *Angew. Chem.* **1995**, *107*, 1470; *Angew. Chem. Int. Ed. Engl.* **1995**, *34*, 1332.
[12] A. Herzog, A. Maderna, G. N. Harakas, C. B. Knobler, M. F. Hawthorne, *Chem. Eur. J.* **1999**, *5*, 1212.
[13] a) L. I. Zakharkin, A. I. Kovredou, V. A. Ol'shevskaya, Zh. S. Shaugumbekova, *J. Organomet. Chem.* **1982**, *226*, 217; b) J. Li, C. M.

Logan, M. Jones, *Inorg. Chem.* **1991**, *30*, 4866; c) G. Barberà, F. Teixidor, C. Viñas, R. Sillanpää, R. Kivekäs, *Eur. J. Inorg. Chem*. **2003**, 1511.
[14] B. T. King, B. C. Noll, A. J. McKinley, J. Michl, *J. Am. Chem. Soc.* **1996**, *118*, 10902.
[15] a) Z. Zheng, W. Jiang, A. A. Zinn, C. B. Knobler, M. F. Hawthorne, *Inorg. Chem.* **1995**, *34*, 2095; b) W. Jiang, C. B. Knobler, C. E. Curtis, M. D. Mortimer, M. F. Hawthorne, *Inorg. Chem.* **1995**, *34*, 3491.
[16] I. B. Sivaer, V. I. Bregadze, *Collect. Czech. Chem. Commun.* **1999**, *64*, 783.
[17] R. M. Chamberlin, B. L. Scott, M. M. Melo, K. D. Abney, *Inorg. Chem.* **1997**, *36*, 809.
[18] C. Viñas, J. Pedrajas, J. Bertran, F. Teixidor, R. Kivekäs, R. Sillanpää, *Inorg. Chem.* **1997**, *36*, 2482; b) C. Viñas, S. Gomez, J. Bertran, F. Teixidor, J. F. Dozol, H. Rouquette, *Chem. Commun.* **1998**, 191; c) C. Viñas, S. Gomez, J. Bertran, F. Teixidor, J. F. Dozol, H. Rouquette, *Inorg. Chem.* **1998**, *37*, 3640; d) C. Viñas, J. Bertran, S. Gomez, F. Teixidor, J. F. Dozol, H. Rouquette, R. Kivekäs, R. Sillanpää, *J. Chem. Soc. Dalton Trans.* **1998**, 2849.
[19] J. N. Francis, M. F. Hawthorne, *Inorg. Chem.* **1971**, *10*, 594.
[20] a) J. Plesek, S. Hermánek, K. Base, L. J. Todd, W. F. Wright, *Collect. Czech. Chem. Commun.* **1976**, *41*, 3509; b) Z. Janousek, J. Plesek, S. Hermánek, K. Base, L. J. Todd, W. F. Wright, *Collect. Czech. Chem. Communn.* **1981**, *46*, 2818.
[21] J. Plesek, S. Hermánek, A. Franken, I. Císarová, C. Nachtigal, *Collect. Czech. Chem. Commun.* **1997**, *62*, 47.
[22] a) I. B. Sivaev, Z. A. Starikova, S. Sjöberg, V. I. Bregadze, *J. Organomet. Chem.* **2002**, *649*, 1; b) P. Selucky, J. Plesek, J. Rais, J. M. Kyrs, L. Kadlecova, *J. Radioanal. Nucl. Chem.* **1991**, *149*, 131; c) J. Plesek, B. Grüner, S. Hermánek, J. Báca, V. Marecek, J. Jänchenová, A. Lhotský, K. Holub, P. Selucký, J. Rais, I. Císarová, J. Cáslavský, *Polyhedron* **2002**, *21*, 975; d) B. Grüner, J. Plesek, J. Báca, I. Císarová, J. F. Dozol, H. Rouquette, C. Viñas, P. Selucký, J. Rais, *New J. Chem.* **2002**, *26*, 1519; e) J. Llop, C. Masalles, C. Viñas, F. Teixidor, R. Sillanpää, R. Kivekäs, *J. Chem. Soc. Dalton Trans.* **2003**, 556; f) F. Teixidor, J. Pedrajas, I. Rojo, C. Viñas, R. Kivekäs, R. Sillanpää, I. Sivaev, V. Bregadze, S. Sjöberg, *Organometallics*, in press .
[23] a) J. Plesek, B. Grüner, J. Báca, J. Fusek, I. Císarová, *J. Organomet. Chem.* **2002**, *649*, 181; b) J. Plesek, B. Grüner, I. Císarová, J. Báca, P. Selucký, J. Rais, *J. Organomet. Chem.* **2002**, *657*, 59.
[24] a) P. K. Hurlburt, R. L. Miller, K. D. Abney, T. M. Foreman, R. J. Butcher, S. A. Kinkead, *Inorg. Chem.* **1995**, *34*, 5215; b) L. Matel, R. Cech, F. Macásek, S. Hermánek, J. Plesek, *Radiochem. Radioanal. Lett.* **1978**, *35*, 241; c) T. E. Paxson, M. K. Kaloustian, G. M. Tom, R. J. Wiersema, M. F. Hawthorne, *J. Am. Chem. Soc.* **1972**, *94*, 4882; d) J. C. Fanning, L. A. Huff, W. A. Smith, A. S. Terell, L. Yasinsac, L. J. Todd, S. A. Jasper, D. J. McCabe, *Polyhedron* **1995**, *14*, 2893.
[25] L. Matel, F. Macásek, P. Rajec, S. Hermánek, J. Plesek, *Polyhedron* **1982**, *1*, 511.
[26] V. I. Bregadze, *Chem. Rev.* **1992**, *92*, 209.
[27] M. D. Mortimer, C. B. Knobler, M. F. Hawthorne, *Inorg. Chem.* **1996**, *35*, 5750.
[28] W. Jiang, D. E. Harwell, M. D. Mortimer, C. B. Knobler, M. F. Hawthorne, *Inorg. Chem.* **1996**, *35*, 4355.
[29] R. N. Grimes, *Carboranes*, Academic Press, New York, **1970**.
[30] a) S. Hermanek, J. Plesek, B. Stibr, V. Grigor, *J. Chem. Soc. Chem. Commun.* **1977**, 561; b) F. Teixidor, C. Viñas, R. W. Rudolph, *Inorg. Chem.* **1986**, *25*, 3339.
[31] a) S. Hermanek, V. Gregor, B. Stibr, J. Plesek, Z. Janousek, V. A. Antonovich, *Collect. Czech. Chem. Commun.* **1976**, *41*, 1492; b) V. I. Stanko, T. A. Babushkina, T. P. Klimova, Y. U. Goltyapin, A. I. Klimova, A. M. Vasilev, A. M. Alymov, V. V. Khrapov, *Zh. Obshch. Khim.* **1976**, *46*, 1071.
[32] Z. Janousek, J. Plesek, S. Hermanek, K. Base, L. J. Todd, W. F. Wright, *Collect. Czech. Chem. Commun*. **1981**, *46*, 2818.
[33] a) D. Reed, *J. Chem. Res.* **1984**, 198; b) T. L. Venable, W. C. Hutton, R. N. Grimes, *J. Am. Chem. Soc.* **1984**, *106*, 29.
[34] a) L. Borodinsky, E. Sinn, R. N. Grimes, *Inorg. Chem.* **1982**, *21*, 1686; b) C. Viñas, J. Bertran, S. Gomez, F. Teixidor, J. F. Dozol, H. Rouquette, R. Kivekäs, R. Sillanpää, *J. Chem. Soc. Dalton Trans.* **1998**, 2849.
[35] C. Viñas, G. Barberà, J. M. Oliva, F. Teixidor, A. J. Welch, G. M. Rosair, *Inorg. Chem.* **2001**, *40*, 6555.
[36] Formally, we are assuming a Co^{III}/Co^{II} couple, although later molecular orbital analyses are indicative of the strong participation of ligand-based orbitals.
[37] M. F. Hawthorne, D. C. Young, T. D. Andrews, D. V. Howe, R. L. Pilling, A. D. Pitts, M. Reintjes, L. F. Warren Jr., P. A. Wegner, *J. Am. Chem. Soc.* **1968**, *90*, 879.
[38] V. Cerný, I. Pavlík, E. Kustková-Maxová, *Collect. Czech. Chem. Communn.* **1976**, *41*, 3232.
[39] Fitting analysis was performed using the Origin 6.0 program, 1991–1999, Microcal (TM) Software, Inc., Northampton (USA).
[40] a) B. S. Furniss, A. J. Hannaford, P. W. G. Smith, A. R. Tatchell, *Textbook of Practical Organic Chemistry*, Longman Scientific & Technical **1989**, p. 392; b) A. J. Gordon, R. A. Ford, *The Chemist's Companion: A Handbook of Practical Data, Techniques and References*, Wiley, **1972**, p. 216.
[41] Y. S. Sohn, D. N. Hendrickson, H. B. Gray, *J. Am. Chem. Soc.* **1971**, *93*, 3603.
[42] R. M. Wing, *J. Am. Chem. Soc.* **1967**, *89*, 5599.
[43] a) W. E. Geiger, D. Brennan, *Inorg. Chem.* **1982**, *21*, 1963; b) W. E. Geiger, *J. Am. Chem. Soc.* **1974**, *96*, 2632.
[44] a) M. F. Hawthorne, *Acc. Chem. Res.* **1968**, *1*, 281; b) L. F. Warren Jr., M. F. Hawthorne, *J. Am. Chem. Soc.* **1968**, *90*, 4823.
[45] A. Appel, F. Jäkle, T. Priermeier, R. Schmid, M. Wagner, *Organometallics* **1996**, *15*, 1188.
[46] Hyperchem Release 7 for Windows (Hypercube Inc.).
[47] L. Borodinsky, E. Sinn, R. N. Grimes, *Inorg. Chem.* **1982**, *21*, 1686.
[48] P. Sivy, A. Preisinger, O. Baumgartner, F. Valach, B. Koren, L. Matel, *Acta Crystallogr. Sect. C* **1986**, *42*, 30.
[49] J. R. Blackburn, R. Nordberg, F. Stevie, R. G. Albrigde, M. M. Jones, *Inorg. Chem.* **1970**, *9*, 2374.
[50] G. M. Sheldrick, SHELXL97, University of Göttingen (Germany), **1997**.

Received: March 20, 2003 [F4970]

